Institut für Veterinärphysiologie
der Vetsuisse-Fakultät Universität Zürich
Direktor: Prof. Max Gassmann
Arbeitsgruppe : Prof. Thomas A. Lutz

(Arbeit unter Leitung von Dr. Melania Osto)

In vivo efficacy of human-derived anti-amylin antibodies in a transgenic mouse model of diabetes mellitus

Inaugural-Dissertation

zur Erlangung der Doktorwürde der
Vetsuisse-Fakultät Universität Zürich

vorgelegt von

Alexandra Durrer

Tierärztin
von Vevey, Schweiz

genehmigt auf Antrag von

Prof. Thomas A. Lutz, Referent

Prof. Wolfgang Langhans, Korreferent

Zürich 2015

Institut für Veterinärphysiologie
der Vetsuisse-Fakultät Universität Zürich
Direktor: Prof. Max Gassmann
Arbeitsgruppe : Prof. Thomas A. Lutz

(Arbeit unter Leitung von Dr. Melania Osto)

In vivo efficacy of human-derived anti-amylin antibodies in a transgenic mouse model of diabetes mellitus

Inaugural-Dissertation

zur Erlangung der Doktorwürde der
Vetsuisse-Fakultät Universität Zürich

vorgelegt von

Alexandra Durrer

Tierärztin
von Vevey, Schweiz

genehmigt auf Antrag von

Prof. Thomas A. Lutz, Referent

Prof. Wolfgang Langhans, Korreferent

Zürich 2015

Summary

Abstract

The aim of this study was to assess the therapeutic efficacy of high affinity human-derived antibodies (NI-203-26C11) showing high affinity against pathologically misfolded forms of human islet polypeptide (hIAPP) in a transgenic homozygous mouse model expressing hIAPP (FVB/N-Tg(Ins2-IAPP)RHF/Soel/J). Transgenic homozygous male mice received weekly intraperitoneal injections of either NI 203-26C11 or phosphate-buffered saline (PBS 10ml/kg), for three months. Hemizygous mice receiving PBS were used as control. The efficacy of the immunotherapy was assessed by determining body weight, plasma levels of insulin and glucose during glucose tolerance tests at different time points and by assessing the hIAPP-derived amyloid load in the pancreas and islet morphology at the end of the three month experimental period.

While hemizygous mice showed no symptoms of spontaneous disease, both groups of homozygous mice, independently of treatment, developed diabetes mellitus due to β-cell death, associated with impaired insulin secretion (hypoinsulinemia). The treatment with NI 203-26C11 did not improve fasting glycaemia or glucose tolerance in homozygous mice compared to the PBS-treated controls. The NI 203.26C11 antibody administration also did not show beneficial effects in preventing or slowing the progression of diabetes in this mouse strain. Nevertheless, the antibody administration was well tolerated and did not elicit any toxic or systemic immunoreaction.

Keywords: Type 2 diabetes, hIAPP, oligomer, fibril, mouse model, immunization

Zusammenfassung

Das Ziel dieser Studie war es, die therapeutische Wirksamkeit von Antikörpern (NI-203-26C11), die eine hohe Affinität gegen pathologisch gefaltet Formen von humanem Islet Amyloid Polypeptide (hIAPP) aufweisen, in einem transgenrn Mausmodell zu untersuchen, das hIAPP exprimiert. Während drei Monaten wurden, transgene männliche Mäuse wochentliche mit NI 203-26C11 oder Phosphat-gepufferter NaCl Lösung (PBS, 10ml/kg) behandelt. Hemizygote Mäuse, denen ebenfalls PBS appliziert wurde, dienten als Kontrolltiere. Die Wirksamkeit der Immunotherapie wurde anhand des Körpergewichts, Plasma-Insulin- und Glukose-Spiegel während eines Glukose-Toleranztests, der hIAPP-Amyloidablagerungen im Pankreas und der Inselmorphologie beurteilt. Während hemizygote Mäuse keine Anzeichen einer Erkrankung zeigen, entwickelten beide homozygoten Gruppen Symptomen des Diabetes mellitus, infolge eines Verlusts von β-Zellen und einer beeinträchtigten Insulin-Sekretion. Die Behandlung mit NI 203.26C11 hatte keine keinen Einfluss auf die Entwicklung der Krankheitssymptome. Trotzdem muss festgehalten werden, dass die Antikörper gut toleriert wurden und keine toxischen oder systemischen Reaktionen verursachten.

Schlüsselwörter: Type 2 Diabetes mellitus, hIAPP, Oligomer, Fibrillen, Maus, Immuntherapie

Introduction

1. Type 2 diabetes, epidemiologic overview

Type 2 diabetes mellitus (T2DM) is one of the most common endocrine diseases diagnosed in humans worldwide, and its prevalence increases as the consequence of changing lifestyle and eating behavior, increasing obesity and decreasing physical activity (S. Wilde et al., 2004). Epidemiological studies estimated that the prevalence of T2DM among the adult population worldwide reached 6.4% in 2010, and is expected to increase up to 7.7% in 2030 (J.E. Shaw, 2009). Not only the prevalence of the disease but also the number of deaths due to diabetes related complications increases, with an estimate of 4.8 million deaths in adults attributable to diabetes in 2012 (L. Guariguata, 2012). Some research suggests that people tend to develop diabetes at an earlier onset which may be a consequence of increased childhood obesity. People with early-onset diabetes tend to suffer from complications linked to the disease at a higher rate and are more likely to die early than patients developing the disease at older age (D.R. Whiting, 2011). T2DM has not only serious implications on health and lifestyle of individuals, but also affects our health systems and the economy, with an estimate of USD 471 billion globally spent on the treatment and management of T2DM in 2012 (L. Guariguata, 2012).

2. Type 2 diabetes, definition and pathogenesis in humans

T2DM is a metabolic disease with multiple etiologies. It is characterized by chronic hyperglycaemia and glucose intolerance with disturbance of carbohydrate, fat and protein metabolism. T2DM is the result of impaired insulin secretion, insulin action, or both. The disease implies long-term damage, dysfunction and failure of various organs. Clinically, the common symptoms include polyuria/polydypsia, weight loss and at later stages blurred vision. The American Diabetes Association (ADA) set reference values for the clinical diagnosis of human non-pregnant patients based on fasting glucose levels and oral glucose tolerance tests. The oral glucose tolerance test consists of assessing glycaemia 2 hours after an oral glucose load of 75g; the reference values are shown in table 1 (American Diabetes Association).

Clinically T2DM is defined and can be diagnosed as follows:

Symptoms of diabetes plus casual plasma glucose concentration ≥200mg/dl (11.1mmol/l). Casual is defined as any time of day without regard to time since last meal. The classic

symptoms of diabetes include polyuria, polydipsia, and unexplained weight loss.
Or
Fasted plasma glucose ≥126mg/dl (7.0mmol/l). Fasting is defined as no caloric intake for at least 8h.
Or
2 hours postload glucose ≥200 mg/dl (11.1 mmol/l) during an oral glucose tolerance test (oGTT). The test should be performed as described by the World Health Organization, using a glucose load containing the equivalent of 75 g anhydrous glucose dissolved in water

Table 1: Criteria for the diagnosis of T2DM, from American Diabetes Association (ADA).

The two major features of the pathogenesis of T2DM are peripheral insulin resistance and β-cell dysfunction; in most instances, prevailing insulin resistance leads to an exhaustion of the insulin secretory capacity of pancreatic β-cells. Together, these contribute to impaired insulin secretion and the inability to maintain euglycaemia without glucose-lowering therapy.

3. Overview of insulin synthesis, secretion and action

Insulin is a peptide hormone produced by the β-cells of the pancreas. It is synthesized as preproinsulin, which contains a 24 amino acid (-aa) residue signal peptide and which is cleaved once entering the endoplasmic reticulum (ER), resulting in the proinsulin peptide. Once folded in the correct conformation, proinsulin is transported to the trans-Golgi network (TGN) where immature secretory granules are formed. The maturation of proinsulin takes place in the secretory granules, through action of endopeptidases. The C-peptide, a 31-aa residue peptide is released, and this results in the insulin A and B peptide chains which are linked by disulfide bonds and form mature insulin. Insulin is stored in the mature secretory granules waiting for metabolic signals and vagal nerve stimulation to be exocytosed (G. Xu et al., 1998). The release takes place in two phases. First phase occurs rapidly after an increase in blood glucose levels. It is triggered when glucose enters the β-cell through the glucose transporter 2 (GLUT2). After glycolysis and activation of the respiratory cycle, the rise in the ATP:ADP ratio leads to the closure of the ATP-sensitive potassium channel. The resulting depolarization opens voltage-gated calcium channels. Increased Ca^{2+} influx causes the activation of phospholipase C, which cleaves the membrane phospholipid inositol 4,5-biphosphate into inositol 1,4,5-triphosphate (IP3) and diacylglycerol. IP3 binds to receptors on the membrane of the ER, opening the IP3-gated channel, which increases further the intracellular Ca^{2+} concentration and allows the secretion of previously synthesized insulin. The second phase consists in a slow, sustained release of newly formed vesicles under the control of non-glucose secretagogues, like amino acids such as arginine or leucine, parasympathetic release of acetylcholine, cholecystokinin

and gastrointestinally derived incretins such as glucagon-like peptide (GLP-1) and glucose-dependent insulinotropic peptide (GIP) (J. Bryan et al., 2005).

Insulin binds to the insulin receptor (IR), belonging to a subfamily of growth factor receptor tyrosine kinases. The activation of the IR initiates two main pathways: the insulin receptor substrate (IRS)/phosphatidylinositol 3-kinase (PI3K) pathway and the Ras/Mitogen activated protein kinase (MAPK) pathway. The former activates a cascade of PI3K-dependent kinases that phosphorylate and activate additional serine/threonine kinases, including the Akt isoforms. The IRS/PI3K pathway is involved in the acute metabolic effects of insulin, such as glucose uptake, glycogen synthesis, inhibition of lipolysis and of protein degradation (D.J. Burks and M.F. White, 2001). The second pathway acts through the formation of complexes between the exchange factor Sos and Grb2. In certain tissues, such as fat or skeletal muscle, this plays a role in growth and proliferation (Y. Kido et al., 2001).

4. Insulin resistance

One of the two hallmarks of T2DM is peripheral insulin resistance, which consists in a defect of insulin-stimulated glucose uptake, mainly in adipocytes and skeletal muscle cells, but probably also in the brain (D.J. Clegg et al., 2011). Insulin sensitivity is influenced by many factors such as genetic (M. Stumvoll et al., 2002; S. Sakagashira et al., 1996), age (M. Chen et al, 1985), acute exercise (R.J. Sigal et al., 2006; S. Bordenave et al., 2008), physical fitness (S.E. Kahn et al., 1990, G. Lazarevic et al., 2006), dietary nutrients (S. Egert et al., 2014), medication such as steroids (J.C. Beard et al., 1984; S.E. Kahn et al., 1989), obesity (M.C. Pouliot et al., 1991; A.N. Peiris et al., 1989) and body fat distribution (B.H. Goodpaster et al., 1999; M. Cnop et al., 2002). While acute exercise and regular physical activity have a positive effect on insulin sensitivity, advanced age, obesity and in particular abundant visceral fat contribute to insulin resistance.

In humans, skeletal muscle is the primary site of insulin-dependent glucose disposal (A. Nandi et al., 2004). Resistance of skeletal muscle to insulin-dependent glucose uptake is an early step in the development of T2DM. Increased fatty acid concentrations elevate intramitochondrial ratios of acetyl CoA/CoA and NADH/NADH+. A rise in these ratios inactivates pyruvate dehydrogenase, increases intracellular citrate concentration and inhibits phosphofructokinase. The resulting increase in glucose-6-phosphate inhibits hexokinase II activity, which leads to elevated intracellular glucose concentrations and a resulting decrease in muscle glucose uptake (P.J. Randle et al., 1965; G.I. Shulman et al., 2000). Accumulation of fatty acid metabolites in muscles and liver, either caused by increased delivery or decreased metabolism, also contributes to insulin resistance (G.I. Shulman, 2000). It is thought that increasing intracellular fatty acid metabolites, such as diacylglycerol, fatty

acyl CoA or ceramides activate a serine/threonine kinase cascade, leading to phosphorylation of serine/threonine sites on insulin receptor substrates (IRS). Serine-phosphorylated forms of these proteins cannot associate with or activate PI3K, resulting in a decreased activation of glucose transport (G.I. Shulman, 2000).

5. β-cell dysfunction

Under normal circumstances, the secretion of insulin by β-cells is modulated by a number of variables, including the route of administration and concentration of glucose (M. Perley et al., 1967; J.D. Bagdade et al., 1967; W.K. Ward et al., 1984), the nature and quantity of secretagogues and systemic insulin sensitivity. In the early stages of T2DM, although acute glucose-induced insulin secretion is impaired, stores of insulin are still preserved, indicating a failure in insulin secretory mechanisms; this may be due to defects in the first phase of insulin release (C.G. Weir et al., 2001). When decompensation occurs, the synthesis and secretion of insulin are impaired. In fact, insulin gene expression decreases while the expression of other metabolites (such as LDH, hexokinase, glucose-6-phosphatase, and the transcription factor c-Myc) and stress genes is increased (G.C. Weir et al., 2000). Hence, in T2DM patients, β-cell mass and function are eventually compromised and fail to compensate for insulin resistance.

Although the nature of the primary β-cell defect stays elusive, once established chronic hyperglycemia and hyperlipidemia seem to exert deleterious effects on β-cell function (R.P. Robertson et al., 2000). Hyperglycemia contributes to glucose desensitization, β-cell exhaustion and glucotoxic β-cell loss (E. Zini et al., 2010). Increased expression of the protooncogene c-Myc has been postulated to reflect a loss of differentiation of β-cells exposed to elevated glucose (J.C. Jonas et al., 1999). The mechanisms of glucotoxicity may also involve activation of chronic oxidative stress, which impairs the transcription of the insulin gene and may lead to apoptosis (Y. Tajiri et al., 1997; T.A. Matsuoka et al., 1997; Y. Ihara et al., 1999). Structural damages can also be found and contribute to β-cell dysfunction.

6. Overview of IAPP action

Islet amyloid polypeptide (IAPP), also called amylin, is a 37-aa peptide that belongs to the calcitonin peptide family. It is initially expressed as an 89-aa preproprotein that includes a 22-aa signal peptide and two short flanking peptides. IAAP is processed in a similar way as proinsulin; the 22-aa signal peptide is removed in the ER. The resulting proIAPP is then transformed to IAPP in the Golgi apparatus and secretory vesicles, after proteolysis and posttranslational modification. After a disulfide bond is formed between cystein residues 2 and 7, the transformation from proIAPP to the

biologically active IAPP is completed (see Fig. 1; J. Wang et al., 2001; S.P. Smeekens et al., 1992; H.W. Davidson et al., 1987; L. Marzban et al., 2004).

IAPP is stored in the halo region of the secretory granules of the β-cell (P. Westermark et al., 1996) and is co-secreted with insulin. Both IAPP and insulin genes contain similar promoter elements and are regulated by transcription factors such as pancreatic and duodenal homebox 1 (PDX1, M. German et al., 1995; H. Ohlsson et al., 1993; H. Watada et al., 1996). As a circulating hormone, IAPP plays an important role in energy homeostasis; it reduces energy intake, increases energy expenditure, and inhibits gastric emptying and postprandial glucagon secretion (T.A. Lutz, 2013); all these functions seem to depend on a hormonal function in the central nervous system (G. Christopoulos et al., 1995; T.A. Lutz, 2013). Binding sites for IAPP have been described in several locations in the brain, notably in the area postrema (AP) and in the nucleus accumbens. IAPP's effect on eating depends on the promotion of meal-ending satiation (T.A. Lutz, 2013; T.A Lutz, 2006; T.A. Lutz et al., 1995). As mentioned, IAPP shares structural similarity with calcitonin. Accordingly, it has been shown that amylin can also inhibit osteoclastic activity and therefore, it may have a physiological role in the inhibition of bone reabsorption (I. MacIntyre, 1989; M. Zaidi et al., 1990, D. Naot et al., 2008).

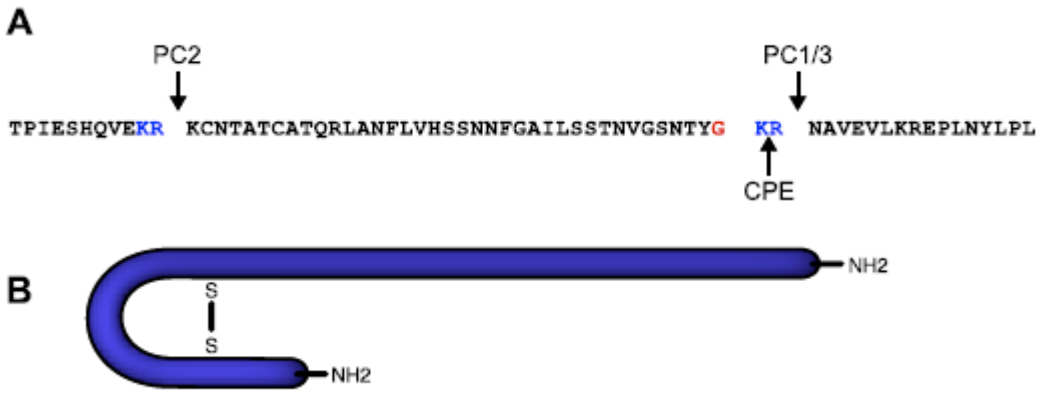

Fig. 1: A. –Amino acid sequence of human proIAPP. Cleavage sites for prohormone convertase 2 (PC2 at the NH_2 terminus) and prohormone convertase 1/3 (PC1/3 at the COOH terminus) are indicated by arrows. KR residues (in blue) are removed by the carboxipeptidase E (CPE).
B. –Structure of mature human IAPP with intramolecular S-S bond between residues 2-7 and the amidated COOH terminus (adapted from P. Westermark et al., 2011).

7. Heterogeneity of IAPP and amyloidogenesis

In general, the aa sequence of IAPP is strongly conserved among mammalian species. Pancreatic amyloid deposition derived from IAPP precipitation, however, has been shown only in humans', other primates' and cats' pancreatic islets. These species express an amyloidogenic region of IAPP

that is essential for amyloid formation and toxicity. Amyloid is a generic term that refers to specific protein aggregations in which the molecules are present in β-sheet conformation and bound to each other, and which leads to a typical light microscopic “amyloid” appearance.

In the case of IAPP, amyloidogenesis seems to be associated with the heterogeneity of the amino acid residues 20-29 in the IAPP sequence. In species where pancreatic amyloid deposition does not occur, like mouse or rat, one or more proline residues can be found in this region. The substitution of proline residues at either position 22, 24 or between 26 and 28 leads to a drastic reduction of amyloid formation (see Fig. 2). It is thought that the presence of proline residues disrupts the ordered structure, like the β-sheet conformation, and subsequently inhibits amyloid aggregation (D.F. Moriarty et al., 1999; C. Betsholtz et al., 1989; A.V. Matveyenko et al., 2006; C. Wu et al., 2013).

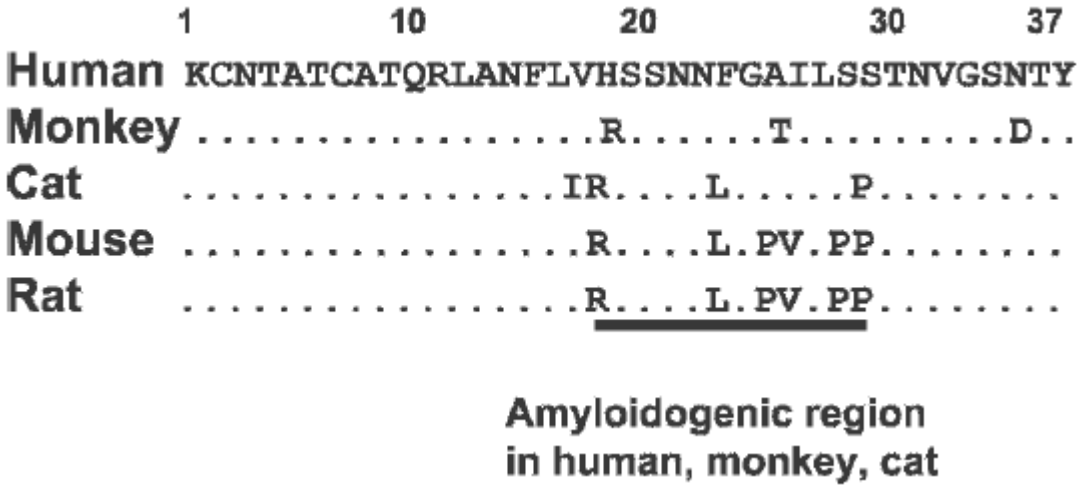

Fig 2: Different sequence in amino acid residues 20-29 in human, monkey, cat, mouse and rat (adapted from A.V. Matveyenko et al., 2006).

8. Amyloid aggregation

Generally speaking, amyloid formation is similar to the build-up of crystals from salts. Starting from an initial nucleation center, crystallization continues to build larger conglomerates. Similarly, the first step in fibril formation is called “the nucleation phase”, in which monomer peptides start to unfold and form a core. The second phase consists in the elongation of amyloid fibrils, while in the third phase, fibrils formation reaches a steady state and the fibrillar mass is constant (A.S. Cohen et al., 1959).

Monomeric IAPP is normally soluble and natively unfolded. It is believed that IAPP is protected from aggregation by interaction with other components within the secretory vesicles like insulin, pro-

insulin or their processing intermediates (P. Westermark et al., 1996). It seems that small changes in the concentration of IAPP in comparison with other halo components can initiate the aggregation and formation of fibrils under certain conditions (J.F. Paulsson et al., 2006). When fibril formation begins, the molecules in β-sheet conformation are bound to each other, predominantly by hydrogen bounds. This β-sheet forms thin and stable layers in which the β-strands are oriented perpendicular to the fibril axis.

Fibril deposition has originally been thought to be mostly extracellular. However, it has been demonstrated that amyloid formation may actually begin within the cell (E.T.A.S. Jaikaran et al., 2001; J. Janson et al., 1996; J.F. Paulsson et al., 2006; G.T. Westermark et al., 2000; K. Yagui et al., 1995). Similarly, studies in insulinoma which may also be associated with IAPP-derived amyloid formation, showed that fibrillogenesis initiates intracellularly (T.D. O'Brien et al., 1994). Further, in addition to mature IAPP, proIAPP and its intermediates may also be amyloidogenic and hence may be the starting point of the aggregation (G.T. Westermark et al., 2000).

No precise localization of the aggregates within the cells has been demonstrated yet. In studies in baboons, amyloid deposits were observed in the cytoplasm as well as bound to the outer β-cell membrane (R. Guardado-Mendoza et al., 2009). In other studies, where islets from diabetic patients were transplanted in nude mice or cultured in vitro, early amyloid formed an intracellular network, suggesting its presence in the ER (J.F. Paulsson et al., 2006; P. Westermark et al., 1995) but also in the Golgi and secretory vesicles (K. Yagui et al., 1995). Finally, prolonged hyperglycemia per se may lead to a higher concentration of proIAPP within the β-cells (X. Hou et al., 1999). This may create a core for further aggregation, ultimately leading to the death of the cell and deposition of extracellular amyloid (J.F. Paulsson et al., 2005).

9. Cytotoxic effect of IAPP oligomers

Islet amyloid formation is a striking abnormality of human T2DM and can be found in more than 90% of T2DM patients (A. Clark and M.R. Nilsson, 2004). Similarly, islet amyloid is a very prominent feature in diabetic cats (T.A. Lutz et al., 2014; T. O'Brien et al., 1993; A.M. Herndon et al, 2014).
The toxicity of amyloid deposition or oligomers may depend on the action of different mechanisms that act together intra- and extracellulary.

9.a. ER stress and unfolded protein response (UPR)

ER stress is an important feature in IAPP-related β-cell toxicity and therefore T2DM pathology. Peripheral insulin resistance triggers β-cells to produce more insulin in parallel with an increased synthesis of IAPP. As these proteins are destined for exocytosis, they are transported through the ER

and trans-Golgi complex and stored in secretory granules before secretion. In the tubular system of the ER, proteins fold into their native structure and undergo posttranslational modifications.

ER stress is characterized by the unfolded protein response (UPR), which is induced to cope with an increase in proteins synthesis or obstruction in the ER-Golgi transport (A.M. Preston et al., 2009). This may e.g. happen during increased IAPP synthesis in early phases of T2DM. UPR consists in the upregulation of ER-located chaperones to assist in the folding of proteins prone to aggregation. Misfolded proteins are then transported to the ubiquitin-proteasome system for degradation. If the homeostasis cannot be reestablished, apoptosis is induced (E.L. Davenport et al., 2008; S.J. Marciniak et al., 2006; S. Oyadomari et al., 2002).

9b. Reactive oxygen species (ROS)

The overexpression of ProIAPP or IAPP in early phases of T2DM characterized by β-cell stimulation with increased insulin and IAPP transcription may lead to the formation of toxic oligomers. These oligomers may enter the cytosol and disrupt the membrane of organelles such as mitochondria resulting in increased cellular oxidative stress and the formation of reactive oxygen species (ROS). Increased ROS levels may ultimately lead to significant damages to cell structures (T. Gurlo et al., 2010; J.K. Parks et al., 2001; R. Scherz-Shouval et al., 2007).

9c. Autophagy

Accumulation of fibrillar material in the halo region of secretory vesicles may lead to a disruption of the vesicles and result in the release of fibrillar material into the cytosol. Because the proteasome pathway can degrade misfolded single proteins but not their aggregates, the latter will be dissolved by the autophagy process. Autophagy is a well-preserved catabolic process that is active in degradation and recycling of misfolded proteins, excess or defective organelles. Autophagosomes fuse with lysosomes, forming autophagolysosomes. Eventually, their maturation is hampered, causing accumulation of material in autophagic vacuoles, disturbing intracellular cell transport (F. Shang et al., 1997; E.L. Davenport et al., 2008; S.J. Marciniak et al., 2006; M. Schröder, 2008). Such a process with an intracellular accumulation of autophagolysosomes has been suggested to induce cell death in pancreatic β-cells (W. Bursch et al., 2000).

9d. Cell membrane damages

The direct toxicity of amyloid for the cell membranes is thought to be mediated by two pathways. On one hand, toxic oligomers can develop and be inserted into the membrane and act like ion-leaking pores (M. Kawahara et al., 2000). On the other hand, misfolded monomers or oligomers can interact

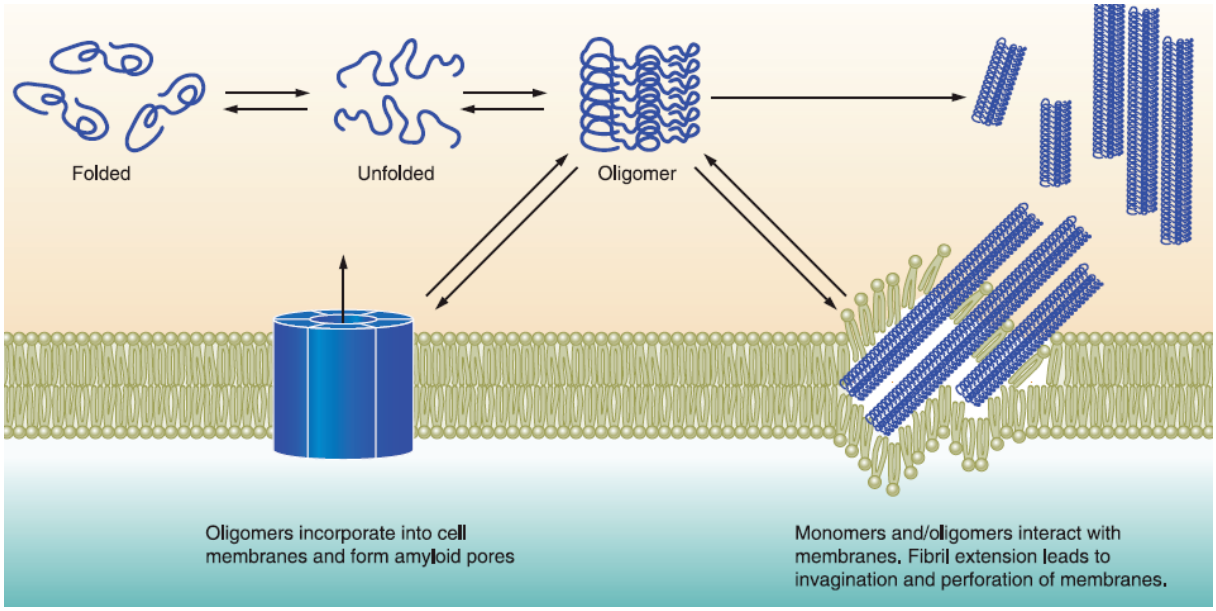

with membrane structures. As these fibrils may continue to grow, they can lead to invaginations and mechanical disruption of the cell membrane, as depicted in Fig. 3 (P.E.S. Smith et al., 2009).

Fig. 3: Scheme representing potential cell toxicity mechanisms linked to amyloid formation in T2DM (adapted from P. Westermark et al., 2011).

9e. Other cytotoxic effects

Finally, aggregated IAPP may activate the inflammasome, a multiprotein oligomer expressed in myeloid cells and components of the innate immune system, to produce interleukine-1β, (IL-1β). This may also lead to β-cell death (M.Y. Donath, 2011; M.Y. Donath, 2013; S.L. Masters et al., 2010; C. Westwell-Roper et al., 2011). IL-1β receptor antagonists have been shown to be beneficial in the treatment of T2DM (M.Y. Donath, 2013). Finally human IAPP can also directly induce apoptosis via activation of acid sphingomyelinase which produces ceramide and which in turn is involved in programmed cell death (Y. Zhang et al., 2009).

10. Islet amyloid deposition and T2DM

Studies in several animal species with naturally occurring IAPP derived-amyloid and in transgenic animals expressing human IAPP demonstrated that islet amyloid formation plays a key role in β-cell apoptosis and dysfunction (A.E. Butler et al., 2004; E.J.P. De Koning et al., 1993; C.F.J. Howard, 1978; C.F.J. Howard, 1986; K.H. Johnson et al., 1989; O'Brien et al., 1985; O'Brien et al., 1986; R. Guardado-Mendoza et al., 2009). A reduction of islet volume due to a decrease in β-cell mass has been associated with increased islet amyloid deposits (F. Wang et al., 2001; P. Westermark et al., 1978). Interestingly, the extent of the amyloid deposition in diabetic humans can vary from very little to 80% of the islets (A. Clark and M.R. Nilsson, 2004). This indicates that in humans, islet amyloid formation may rather be a result of diabetes-related pathologies than a single etiological factor. On the other hand, it has been shown that the progressive increase in small perivascular amyloid

deposits correlates with progressive β-cell dysfunction in rodent models as well as in obese cats and monkeys (A. Clark and M.R. Nilsson, 2004). Similar correlations have also been observed in humans, where progressive β-cell destruction was associated with severe islets damage and increased insulin requirements to control glycaemia (A. Clark and M.R. Nilsson, 2004). Therefore, whether IAPP deposition is a primary cause or a consequence of T2DM still remains somewhat controversial.

11. Strategies against amyloid formation

Several strategies to block various key steps in amyloidogenesis are currently pursued. One strategy consists in the inhibition of the expression of the amyloidogenic protein itself, for example by using anti-sense DNA. Although this approach shows promising results *in vitro*, blocking a natural protein or peptide that plays important biological functions might not be safe *in vivo* (F.G. De Felice et al., 2002; K.A. Conway et al., 2003) and it may be difficult to maintain the effect over extended periods. In fact, the lack of circulating IAPP seems to be responsible for pathologically accelerated gastric emptying and exaggerated postprandial release of glucagon that may contribute to postprandial hyperglycemia, as shown in patients suffering from type 1 diabetes (H.J. Woerle et al., 2008) but also T2DM. Another strategy using small organic ligands, such as N-phenyl phenoxazines and flufenamic acid derivates, aims at stabilizing the native form of the amyloidogenic peptide (M.G. McCammon et al, 2002).

In other amyloid-associated diseases, such as Alzheimer disease (AD), the precursor protein has to be cleaved by enzymes to form amyloidogenic peptides. Drugs targeting the inhibition of these enzymes are interesting targets in the management or prevention of amyloid deposition. However, this approach would not be helpful in the case of T2DM because it is the full length peptide that is amyloidogenic (C. Haass and B. De Strooper et al., 1999).

Other treatments designed to inhibit the aggregation of proteins either by using small ligands or indirectly by immunization are under consideration. The latter treatment strategy may not be able to prevent the initial formation of oligomers or insoluble fibers and may be less effective than strategies targeting the steps prior to protein aggregation. Nonetheless, the inhibition of the aggregation is an attractive therapeutic strategy as it is not supposed to interfere with the natural biological function of the underlying peptide (J.M. Mason et al., 2003).

12. Immunotherapy against toxic aggregates of IAPP

Immunotherapy against amyloid deposition has been successfully developed for several brain diseases involving protein aggregation such as Alzheimer's disease, Parkinson's disease, and

amyotrophic lateral sclerosis (H. Jindal et al., 2014; D.R. Shprecher et al., 2013; K. Marciniuk et al., 2013). Alzheimer's disease (AD) shares several pathophysiological features with T2DM that underlie the respective degenerative developments of neurons or β-cells, respectively (L. Li and C. Hölscher, 2007). These include aging-related processes, high cholesterol levels, metabolic disorders and β-amyloid aggregation. Besides the fact that both diseases show disturbances in insulin, insulin growth factors and transforming growth factor signaling, the misfolding of proteins plays an important role in AD as well as in T2DM (M. Romano et al., 2003; I. Tesseur et al., 2006; C. Hölscher, 2005, D.H. Small and R. Cappai, 2006; A. Clark et al. 1988; S. Mohanty et al., 2005; H.D. Venters et al., 2001). Thus, at the structural level, amyloid polypeptide (APP) derived amyloid deposition in AD shares 90% similarities with IAPP derived amyloid found in T2DM (J. Janson et al., 2004).

In 2000, Games et al. published a study on the effects of intraperitoneal administration of antibodies against Aβ-plaques in a mouse model for Alzheimer's disease. PDAPP mice were used which are transgenic for an amyloid β precursor protein mini-gene driven by a platelet growth factor promoter (D. Games et al., 2000). These mice overproduce the highly amyloidogenic $A\beta_{1-42}$ peptide relative to other Aβ peptides and show many of the pathological features of Alzheimer disease, including extensive deposition of extracellular amyloid plaques in the cortex and hippocampus, astrocytosis and neural dystrophy (D. Games et al., 1995; E. Masliah et al., 1996). Monoclonal antibodies against Aβ plaque bound to amyloid aggregates. Injected antibodies were found in the brain, indicating that the antibodies were able to cross the blood-brain barrier and to enter the central nervous system to reach plaques. Interestingly, the antibodies reduced the plaque burden by about 80% in the cortex. The passive immunization with exogenous antibodies against Aβ did not result in a T-cell proliferative response to Aβ. Ex vivo assays with sections of brains from PDAPP mice or deceased Alzheimer patients indicated that the antibodies triggered microglial cells to clear plaques through Fc receptor-mediated phagocytosis and subsequent peptide digestion. A T-cell response did not seem to be required for amyloid plaque clearance; in other words, the antibodies appeared to be sufficient to decrease amyloid deposition in PDAPP mice. In another study (C. Hock et al., 2003), active immunization was tested in human patients suffering from mild to moderate forms of Alzheimer disease. These patients received active prime and booster immunizations with preaggregated $A\beta_{1-42}$ or placebo, in a double-blind, randomized study design. The patients who generated antibodies specifically recognizing β-amyloid plaques performed markedly better on the Mini Mental State Examination (MMSE) and had significantly better Disability Assessment for Dementia (DAD) rating.

These clinical studies suggested that immunization against toxic oligomers may have beneficial effects in slowing the clinical and the cognitive decline of patients with AD. Similar approaches may

therefore be promising in the treatment of other diseases associated with amyloid aggregation, in particular T2DM.

13. Animal models of Type 2 Diabetes

To study the pathophysiology of pancreatic dysfunction in T2DM, longitudinal studies of the pancreas morphology in humans are not possible. Usually, human tissue is only available at the time of autopsy or during surgical resection of pancreatic cancers. This may lead to problems like post mortem autolysis or altered islet function and anatomy in the case of cancer (M. Shimizu et al. 1990; P. Fogar et al., 1994). The study of species like non-human primates and cats that naturally express amyloidogenic IAPP and that may spontaneously develop diabetes is complicated by ethical issues, by the relatively slow progression of the natural disease, by the small and unpredictable number of individuals who may actually suffer from the disease (Howard et al., 1986; T.D. O'Brien et al., 1993) and by the high housing and maintenance costs of experimental animals (A.V. Matveyenko et P.C. Butler, 2006).

Traditionally, some of the most common rodent models used for longitudinal studies to study some aspects of T2DM were the db/db mouse and the diabetes-prone Zucker diabetic fatty rat (ZDF). Both models are characterized by mutations of the leptin receptor (H. Chen et al., 1996; M.S. Philips et al., 1996). Ob/ob mice, carrying a mutation in the leptin gene, were also used (M.A. Pelleymounter et al., 1995). Both receptor-deficient and leptin deficient models develop severe obesity with sudden onset of hyperglycaemia (F. Kawasaki et al., 2005; Y. Lee et al., 1994; D.T. Finegood et al., 2001; A. Pick et al., 1998; E. Shafrir et al., 1999; T. Tomita et al., 1992).

However, these rodent models do not fully mimic the pathological features of human T2DM. In particular, amyloid deposition is not present because rodent IAPP is not amyloidogenic, and animals require an extreme obese phenotype to eventually develop diabetes. Other rodent models include the high calories-fed sand rat (Psammomys obesus) and the Goto Katazaki rat (GK rat). The sand rat develops insulin resistance and hyperglycemia within few days when fed high energy diet. Although an extreme obese phenotype is not needed to provoke diabetes, this rat model also does not develop amyloid deposition (E. Shafrir and A. Gutman, 1993; M.Y. Donath et al., 1999). The GK rat is a non obese rat having decreased β-cell mass at birth due to defective β-cell proliferation (B. Portha et al., 2001; J. Movassat et al., 1997). It is characterized by a slight increase in fasted glucose due to impaired insulin secretion and by the presence of insulin resistance in liver and skeletal muscles. As in the other rodent models, however, there is no amyloid deposition in the islets (F. Picaret-Blanchot et al., 1996).

The lack of amyloidogenesis in all these rodent models of T2DM is due to the absence of amyloidogenic sequence in the rodent IAPP. To investigate the pathogenic effects of amyloid formation and to test targeted treatment in vivo, transgenic mice and rats carrying human IAPP were generated. The first mouse model was the hemizygous FVB/N-Tg(Ins2-IAPP)RHF/Soel/J mouse that is transgenic for human IAPP; these mice developed diabetes only if treated with dexamethasone and growth hormone for one month in order to induce marked insulin resistance (M. Couce et al., 1996; E.J. De Koning et al., 1994, K. Yagui et al., 1995). These mice showed evidence of β-cell degeneration and small intra- and extracellular amyloid deposition.

In 1996, Janson et al. generated a new hIAPP transgenic mouse model, the homozygous FVB/N-Tg(Ins2-IAPP)RHF/Soel/J mouse (J. Janson et al., 1996). In homozygous male mice, diabetes developed spontaneously, at 4 - 8 weeks of age due to rapid β-cell death, impaired insulin secretion and hyperglycemia. If untreated, male mice died around 16 weeks of age, as a consequence of severe hyperglycemia. Interestingly, only small intracellular IAPP aggregates were present that could be detected by electron microscopy. The homozygous females developed a much milder phenotype, including mild hyperglycemia by 16 weeks of age (see Table 2). Because their plasma insulin levels were similar to those of wild type females, the authors suggested a defect in insulin secretion in the homozygous male mice (J. Janson et al., 1996). The sexual dimorphism may rely on divergent effects of estrogens versus androgens on hepatic estrogen sulfotransferase. Androgens may cause relative insulin resistance in male mice (A.M. Gill et al., 1994) and may therefore contribute to the faster progression of diabetes in males.

MICE hIAPP/FBV/N	Hemizygous	Homozygous
Phenotype	Normal weight	Normal weight (or slightly decreased) Sexual dimorphism
Diabetes development	Do not develop diabetes spontaneously	Male: Onset: 4-8 wk Death: 16 wk Female: Onset: ≥30 wk (in 20%)
Plasma levels		Male: 8-16 wks: ↑IAPP ↓Insulin ↑Glucose Female 14-16 wks: ↑ IAPP ↑Glucose
Islet pathology	β-cell degeneration	abnormal islet morphology ↓ β-cell mass, number β-cell degeneration
Pancreatic Amyloid	In insulin resistant mice: perivascular extracellular Congo Red + deposits visible with light microscopy	Intra-and extracellular amylin deposits. Fibrillar aggregates (5-26 wk) visible with electron microscopy

Table 2: Summary of differences between homo- and hemizygous FVB/N-Tg(Ins2-IAPP)RHF/Soel/J mice, wk = week, ↑= increased, ↓= decreased (adapted from M. Couce et al., 1996; J. Janson et al., 1996)

Other human IAPP transgenic mouse models were generated by cross-breeding hemizygous FVB/N-Tg(Ins2-IAPP)RHF/Soel/J mice with obese Avy/Agouti or ob/ob mice The resulting mice showed an increased expression of the human-IAPP, developed diabetes and islet amyloid deposition (A.E. Butler et al., 2003; Hoppener et al., 1999; Soeller et al., 1998). Hemizygous FVB/N-Tg(Ins2-IAPP)RHF/Soel/j mice were also cross with C57BL/6 x DBA mice. If fed a high fat diet, these mice developed diabetes and showed evidence of decreased β-cell mass and presence of extracellular amyloid deposits; the DBA background may have caused an increased susceptibility to dietary fat-related factors and an increased insulin and hence IAPP release (R.L. Hull et al., 2005; F. Wang et al., 2001)

A human IAPP transgenic rat model has also been generated on a Sprague Dawley background, the HIP rat (A.E. Butler et al., 2004). Homozygous rats develop diabetes rapidly within 2 months of age without extracellular amyloid deposition, while hemizygous developed the disease at older age (6-12 months of age) with the presence of extensive amyloid deposits (A.E. Butler et al., 2004).

In summary, these transgenic rodent models may be more useful for the study of T2DM than traditionally used models. Differences in the genetic background as well as the rate of expression of the transgene may be responsible for the variable phenotypes, including differences in the presence of visible amyloid deposits.

Aim of the study

In the current study, a passive immunotherapy targeting toxic aggregates of IAPP was tested in FVB/N-Tg(Ins2-IAPP)RHF/Soel/J homozygous mice. Human anti-hIAPP antibodies showing high in vitro binding selectivity and affinity against hIAPP aggregates were first isolated from blood of healthy human donors, cloned, purified and characterized in order to be administered intraperitoneally in our mouse model.

Our aim was to study the therapeutic efficacy of the anti-hIAPP antibodies to slow diabetes progression in this transgenic mouse model of T2D expressing human IAPP. The efficacy of the immunotherapy was assessed by determining plasma levels of insulin and glucose during glucose tolerance tests, together with hIAPP amyloid load in the pancreas.

Materials and methods

1. Preparation of transgenic construct

The RIPHAT transgene construct was produced with PCR-generated cDNA of the human IAPP coding sequence under the regulatory control of the rat insulin II *ins2* promoter/5'UTR (untranslated leading region) and the human albumin intron I. It was followed by polyadenylation signal /RNA termination region from the glyceraldehydes-3-phosphate gene and 3'UTR, as shown in Fig. 4 (M. Couce et al., 1996; J. Janson et al., 1996).

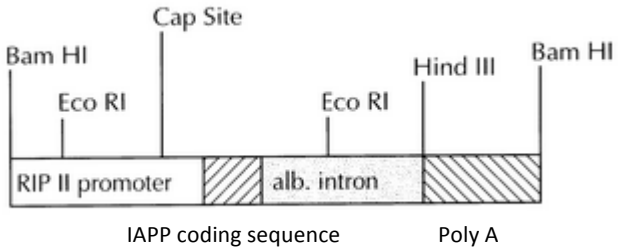

Fig 4: Restriction map of the RIPHAT transgene (2395 bp): PCR-generated cDNA human IAPP coding sequence (first striped box); RIP II promoter, the rat ins2 promoter and 5'UTR (white box). Alb. intron, human albumin intron I (light-shaded); poly A, polyadenylation signal /RNA termination region from the glyceraldehydes-3-phosphate gene and 3'UTR (second striped box). Bam HI, Eco RI and Hind III are type II restriction endonuclease isolated from Bacillus amyloli, Escherichia coli and Hemophilus influenza, respectively (adapted from W.C. Soeller et al., 2001)

2. Generation of transgenic mice

FVB/N-Tg(Ins2-IAPP)RHF/Soel/J (JAX stock 008232) transgenic mice were generated and characterized at Jackson Laboratory (Bar Harbour, USA), as previously described (M. Couce et al., 1996; J. Janson et al., 1996; W.C. Soeller et al., 2001). The entire RIPHAT transgene was cloned into plasmid pBluescript to generate pRIPHAT1. The pRIPHAT1 was digested with endonuclease BamHI, followed by agarose electrophoresis, electroelution of the DNA from the gel slice, and purification on a Schleicher and Schuell Elutip column, in order to obtain a 2.4kb linear DNA fragment, ready for microinjection. The DNA fragment was then microinjected in pronuclei of FVB/N fertilized oocytes, which were implanted in pseudogravid females to produce fertile offspring expressing the hIAPP. The FVB/N inbred mouse strain was chosen as background to produce the transgenic animals because it is known that this strain is preferable for transgenic experiments and analyses. The phenotype of these mice shows fertilized ovocytes with large pronuclei, which facilitates DNA microinjection (see Fig. 5; Taketo et al, 1991). Founder animals were identified by PCR amplification of transgene sequences from tail DNA. The RHF transgenic line, the founder line, was selected based on their higher level of RNA expression of hIAPP in the pancreas. High resolution mapping of the transgene in prometaphase spreads of endoreduplicated cells indicates the transgene insertion at a single location on chromosome 15 (15C).

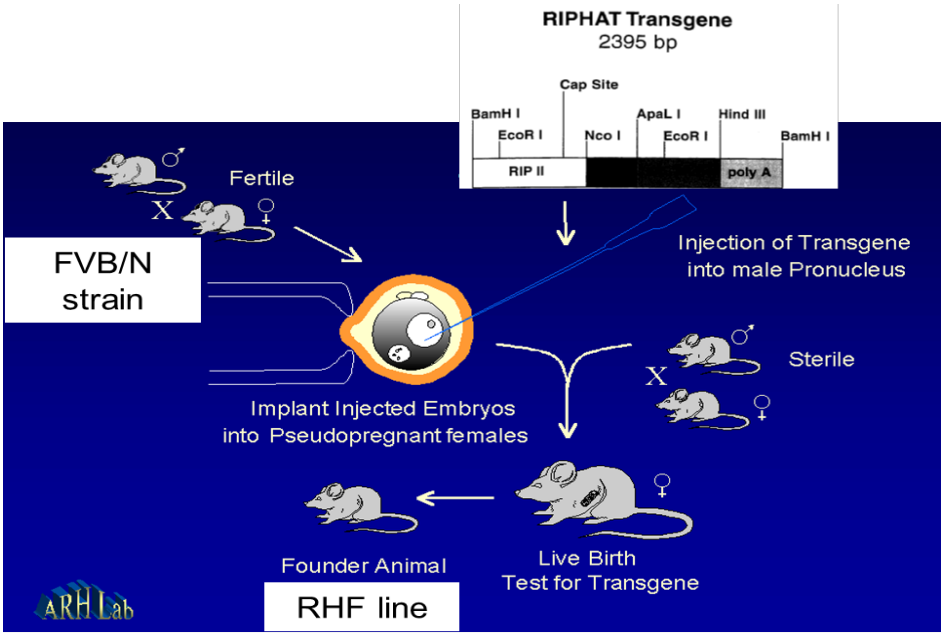

Fig 5: Scheme representing the production of transgenic mice.
(Adapted from M. Couche et al. 1996; and from the web site of the Department of Nutrition & Food Science at Wayne State University, clasweb.clas.wayne.edu/NFS)

2a. Breeding plan

For the current study, breeding pairs of transgenic FVB/N-Tg(Ins2-IAPP)RHFSoel/J (JAX stock No. 008232) mice were purchased from Jackson Laboratory (Bar Harbor, USA). Two matings were performed by crossing hemizygous males (FVB (hIAPP) tg/-; n=8) with hemizygous females (FVB (hIAPP) tg/-; n=15), following a trio mating scheme (one male with two to three females). Transgenic offspring was identified by PCR amplification of the RIPHAT from ear DNA as described by Couce (M. Couce et al., 1996). Hemizygous mice were distinguished from homozygous by quantitative PCR. After the first mating, 23 transgenic males (hemizygous n=17; homozygous n=6) and 22 transgenic females (hemizygous n=16; homozygous n=6) were obtained. Homozygous mice were also generated using a homozygous female x homozygous male breeding scheme. After two matings using three homozygous breeding pairs, 19 homozygous females and 25 homozygous males were generated. Mice received water and conventional chow diet ad libitum (Kliba Nafag 3436, Provimi Kliba AG, Kaiseraugst, CH) and were kept on a 12 hours light/dark cycle. F1 and F2 male offspring were used in the experiment. All animal experiments have been approved by the Cantonal Veterinary Office of Zurich, Switzerland (licence #121/2012).

3. Genotyping

3a. DNA extraction

At two weeks of age, ear biopsies were taken from the mice to perform the genotyping.
Tissues were lysed using 20mg/ml Proteinase K (Promega, Madison, USA) and 2XPK buffer (200mM Tris-HCl pH 7.5, 2.5mM EDTA, 300mM NaCl, 2% SDS). The DNA was purified by centrifugation with phenol-chloroform (Carl Roth, Arlesheim, CH), precipitated with ethanol and sodium acetate (pH 5.5) washed again with ethanol and resuspended in TE buffer (Tris-EDTA buffer, pH 8.0, Promega).

3b. Standard PCR

After DNA extraction, the presence of the hIAPP transgene in the offspring was determined by PCR. This technique differentiates transgenic carriers from wild type mice but does not allow to distinguish between homo- and hemizygous Amplification was performed by Go Taq DNA polymerase (5 U/µl, Promega). The PCR reaction mixture is reported in Table 3.

Products	Quantity
10x AB PCR Buffer (Applied Biosystems, Zug, CH)	1.20 µl
25 mM MgCl2 (Applied Biosystems)	0.96 µl
2.5 mM dNTP (Promega)	0.96 µl
20 µM Transgene Forward	0.60 µl
20 µM Transgene Reverse	0.60 µl
20 µM Internal Positive Control Forward	0.25 µl
20 µM Internal Positive Control Reverse	0.25 µl
5 mM DNA Loading Dye (Promega)	1.66 µl
5 U/µl Taq DNA polymerase (Promega)	0.06 µl
ddH_2O (Qiagen, Hilden, DE)	3.46 µl
DNA sample	2.00 µl

Table 3: Quantity of reagents used for the amplification of one sample in the PCR reaction.

Primers for the genotyping of the hIAPP gene are reported in Table 4. The reaction mixture also included primers for an internal positive control, which consists of primers that amplify a genomic DNA region, the mouse interleukin 2 (IL2) gene that is unrelated to the transgene (see Table 4). Successful amplification of the internal control indicates that the DNA is suitable for the PCR. All primers were purchased from Microsynth (Balgach, CH).

Sequence (from 5' to 3')	Primers
CTA GGC CAC AGA ATT GAA AGA TCT	Internal positive control forward (Il-2)
GTA GGT GGA AAT TCT AGC ATC ATC C	Internal positive control reverse (Il-2)
GTC ATG TGC ACC TAA AGG GGC AAG TAA TTC A	IAPP transgene forward
CGA GTG GGC TAT GGG TTT GT	IAPP transgene reverse

Table 4: Primers and respective sequence used for the PCR reaction.

The Thermal cycle reaction was set as shown in Table 5. All PCR reactions were carried out with Personal thermocycler instrument (Biometra GmbH, Goettingen, Germany).

Cycling Step #	Temperature °C	Time	Notes
1	94	3 min	Melting
2	94	30 sec	Denaturation
3	63	1 min	Annealing
4	72	1 min	Extension Repeat 2-4 for 35 cycles
5	72	2 min	

Table 5: Settings for the PCR program.

3c. Agarose gel electrophoresis

2g of agarose (MP Biomedicals, Santa Ana, USA) were dissolved in 100ml Tris-acetate-EDTA (TAE) buffer and heated in the microwave for approximately 1.5 minutes. After cooling the solution for 5

minutes, 5µl of Roti-safe dye (Carl Roth, Karlsruhe, Germany) were added and mixed to the solution. While still fluid, the gel was poured into a clean gel mold and a fitting comb was inserted.

After solidification, the gel was transferred into the electrophoresis chamber, which was filled with TAE buffer until the entire gel was covered. After removing the comb, the PCR products were carefully loaded in the gel wells (12µl for each sample). A 100bp DNA ladder was used (Gene ruler 0.5 µg/µl, Fermentas, Wohlen, CH). Electrophoresis was run at 140 V for 40 min. DNA bands migration was observed under UV illumination with Biorad UV Light and Gel Documentation Hood (Life Science Group Switzerland, Reinach, CH).

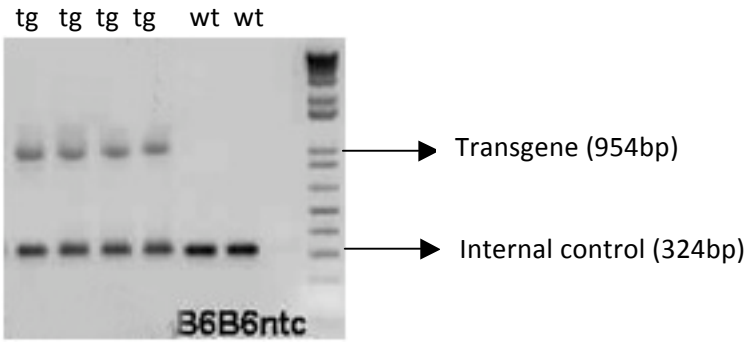

Fig 6: Example of agarose gel. Transgene and Internal Positive Control have a length of approximately 954 bp and 324 bp, respectively. A 100bp DNA ladder scale was used. *(Adapted from the Jackson Laboratory website, http://jaxmice.jax.org/strain/008232.html)*

3d. Quantitative PCR (qPCR)

Quantitative PCRs were performed to differentiate homo- from hemizygous mice. The transgene expression was calculated for each animal that was recognized as transgenic. DNA samples were diluted 1:10. The qPCR reaction was prepared as shown in table 6.

Products	Quantity
2x KAPA Probe fast qPCR	10 µl
40 uM 12855 (transgene forward)	0.28 µl
40 uM 12856 (transgene reverse)	0.28 µl
40 uM oIMR1544 (reference gene forward)	0.28 µl
40 uM oIMR3580 (reference gene reverse)	0.28 µl
5 uM 12857 (transgene probe)	0.81 µl
5 uM TmoIMR0105 (reference gene probe)	0.81 µl
DNA (1:10)	5 µl

Table 6: Quantity of reagents used for the amplification of one sample in the qPCR reaction.

Primers and probes were purchased from Microsynth (see Table 7). The internal control primer and probe set amplify a fragment of the Apoprotein B mouse gene (ApoB). The reaction requires a hybridization probe labeled with two fluorescent dyes. One dye is a reporter dye (FAM) and the other is a quenching dye (black hole quencher, BHQ). When the probe is intact, fluorescent energy transfer occurs and the reporter dye emission is absorbed by the quenching dye. During the extension phase of the PCR cycle, the fluorescent hybridization probe is cleaved by the 5'-3' nucleolytic activity of the DNA polymerase. When the probe is cleaved, the reporter dye emission is no longer transferred efficiently to the quenching dye, resulting in an increase of the reporter emission spectra. Fluorescence is measured with time and corresponds to the amplification of the corresponding gene sequences. This is converted in cycle threshold (CT) values.

Sequence (from 5' to 3')	Primers and probes
CAG CGC CTG GCA AAT TTT	IAPP transgene forward
GCA TTC CTC TTG CCA TAT GTA TTG-3'	IAPP transgene reverse
FAM-CCA CGT TGG TAG ATG AGA GAA TGG CAC-BHQ1	IAPP Transgene probe
CAC GTC GGC TCC AGC ATT'	ApoB gene forward (internal positive control)
TCA CCA GTC ATT TCT GCC TTT G	ApoB Gene reverse (internal positive control)
Cy5- CCA ATG GTC GGG CAC TGC TCA A-BHQ2	ApoB gene probe (internal positive control)

Table 7: Primers and probes used for the qPCR.

The comparative cycle threshold (CT) method, also known as the $2^{-\Delta\Delta Ct}$ method, was used for quantification. The threshold on amplification curves is set based on the variability of the base-line data. Ct values were exported and used for calculating the genotypes. For the analysis, ΔΔCt of the reference gene and the transgene were used. Mean Ct values and standard deviations of the four measurements for the reference gene and the transgene were calculated as follows:

Zygosity factor (Z) = $2^{-\Delta\Delta Ct}$

$$Z = \frac{2^{-(Mean\ Ct\ Ref\ gene\ sample\ 1 - Mean\ Ct\ Ref\ gene\ Controle\ sample)}}{2^{-(Mean\ Ct\ transgene\ sample\ 1 - Mean\ Ct\ transgene\ Controle\ sample)}}$$

A heterozygous control sample was used as reference sample for each calculating ΔΔCt.

An unknown sample with a zygosity factor approaching 1 or 2 was analyzed as hemizygote or as homozygote, respectively.

All qPCR reactions were carried out in the 7500 Real Time PCR System thermocycler instrument from Applied Biosystems (Foster, USA). The thermal cycle reaction for the qPCR was set as shown in Table 8.

Cycling step #	Temperature °C	Time	
1	95	10 minutes	
2	95	15 seconds	Repeated 2-3 for 40 cycles
3	60	1 minute	

Table 8: Settings for the qPCR program.

4. Study design

4.a. Injection protocol

A total of 40 male mice (homo- and hemizygous mice) were included in the experiment (see Table 9). The experiments were run in three series under identical experimental conditions. Hemizygous mice were used as control group (hemi-PBS) to establish reference baseline values. Hemi-PBS (n=10) were injected weekly intraperitoneally (i.p.) with phosphate buffered saline (PBS, pH 7.4, 10ml/kg, Gibco, Auckland, NZ). Homozygous mice were randomly assigned to homozygous-PBS (homo-PBS, n=14) or experimental homozygous-antibody (homo-AB, n=16) groups and then administered PBS (10ml/kg) or human anti-hIAPP antibodies (10mg/kg murinized NI-203.A), respectively. I.p. injections were started in all mice at four weeks of age, and were repeated weekly until the end of the experiment at three months of age. Body weight was measured weekly. Intraperitoneal glucose tolerance tests (ipGTTs) were performed at one, two and three months of age. The ipGTT at one month of age was performed just before any treatment was started and served as baseline. Fasting glucose and insulin levels were measured before every ipGTT.

	Hemizygous-PBS (Hemi-PBS)	Homozygous-PBS (Homo-PBS)	Homozygous-antibody (Homo-AB)
Set 1	0	5	6
Set 2	7	6	7
Set 3	3	3	3
Total	10	14	16

Table 9: Total number of mice used in the experiment.

4b. Human anti-IAPP antibodies

Human anti-IAPP antibodies were produced by Neurimmune Holding AG (Schlieren, CH). Reactive memory B-cells were isolated from the blood of healthy human patients. Antibodies in conditioned media of human memory B cell cultures were screened in parallel for binding to aggregated hIAPP protein and absence of binding to bovine serum albumin (BSA) using a direct ELISA approach. Only B-cell cultures positive for aggregated hIAPP protein but not for BSA were subjected to antibody cloning. Selected relevant antibodies were recombinantly produced and characterized for their binding specificities towards aggregated or non-aggregated hIAPP protein. Antibody selection and characterization was performed by direct ELISA on 96-well plates (Costar, Corning, USA) coated with human IAPP solution or BSA (Bovine Serum Albumin, Sigma-Aldrich, Buchs, Switzerland) diluted to a concentration of 10 µg/ml in carbonate buffer (15 mM Na_2CO_3, 35 mM $NaHCO_3$, pH 9.42). After overnight incubation at room temperature, non-specific binding sites were blocked for 1 hour at room temperature with PBS/0.1% Tween-20 (polysorbate surfactant) containing 2% BSA (Sigma-Aldrich, Buchs, Switzerland). B-cell conditioned medium or recombinantly produced antibodies were transferred to ELISA plates and incubated for one hour at room temperature. ELISA plates were washed in PBS-Tween 20 and binding was determined using horseradish peroxidase (HRP)-conjugated anti-human IgG polyclonal antibodies (Jackson ImmunoResearch, Newmarket, UK). HRP activity was assessed with standard colorimetric detection using a plate reader (Sunrise microplate absorbance reader, Tecan Group Ltd, Männedorf, Switzerland).

In case B-cell conditioned medium showed antibodies with selective binding to aggregated hIAPP protein, mRNA of B-cells was prepared and immunoglobulin heavy and light chains were cloned with a nested PCR approach. The PCR approach consists in a modified polymerase chain reaction intended to reduce non-specific binding in products due to the amplification of unexpected primer binding sites.

Antibodies were identified by rescreening on ELISA upon recombinant expression of complete antibodies in CHO (Chinese Hamster Ovary) cells and using expression vectors, where variable heavy and light chain sequences “in the correct reading frame” were inserted. An Ig-heavy-chain expression vector and a kappa or lambda Ig-light-chain expression vector were used. The monoclonal antibodies were purified with standard protein A column purification and tested again for their binding properties by ELISA.

Figure 7 shows direct ELISA results of the recombinant human NI-203.26C11 antibody. Figure 8 shows an electron microscopy picture of the aggregated hIAPP solution used for the direct ELISA assay andFigure 9 shows fibrillar and non fibrillar IAPP solutions.

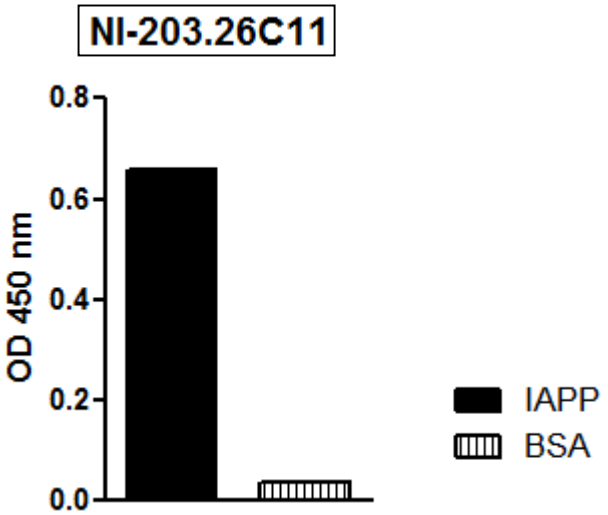

Fig. 7: Results of direct ELISA assay showing binding selectivity of the human NI-203.26C11 recombinant antibody against hIAPP aggregates (IAPP), with no binding to BSA. Data are expressed as optical density values measured at 450 nm (Data from Neurimmune).

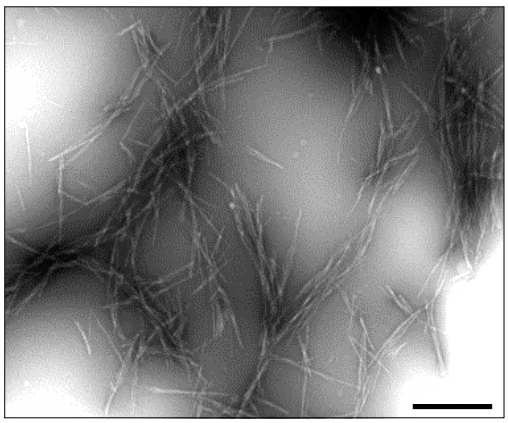

Fig 8: Electron microscopy picture of the aggregated hIAPP solution (2 mg/ml) used for the direct ELISA assay. Full-length human IAPP peptide (1-KCNTATCATQRLANFLVHSSNNFGAILSSTNVGSNTY-37; C-term modification: amide) was purchased from Anaspec (Fremont, CA, USA). The IAPP solution was prepared by dissolving native human IAPP in DMSO for 24 hours at room temperature with shaking (40 rpm). Scale bar represents 1 µm (Data from Neurimmune).

After standard colorimetric detection on a plate reader, the EC_{50} values were estimated by a non-linear regression using GraphPad Prism (San Diego, USA) software, as shown in Fig 10.

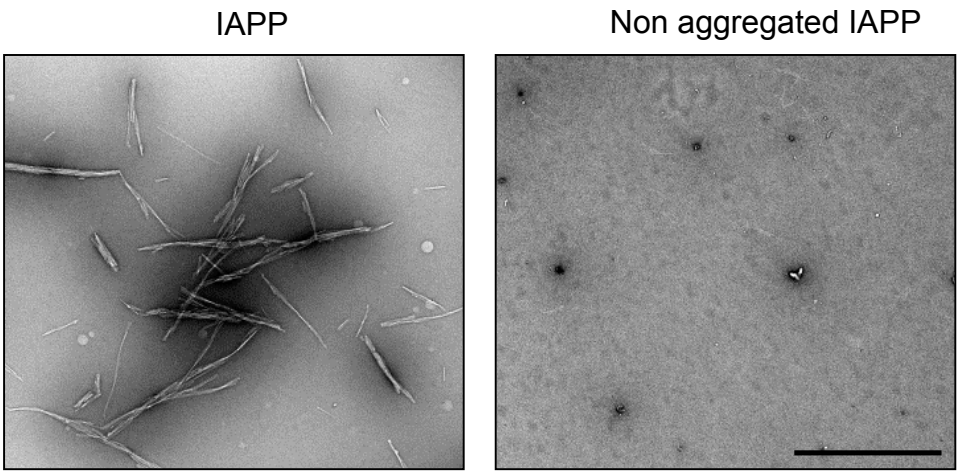

Fig. 9: Electron microscopy images of aggregated human IAPP (IAPP, 2 mg/ml) and non aggregated IAPP (2 mg/ml) solutions used for ELISA plate coating. While the IAPP solution contains clearly visible fibrils, IAPP fibrils are absent in the non aggregated IAPP solution. The non aggregated IAPP solution shows small particles most likely corresponding to small-size IAPP oligomer species. Scale bar represents 1 µm (Data from Neurimmune).

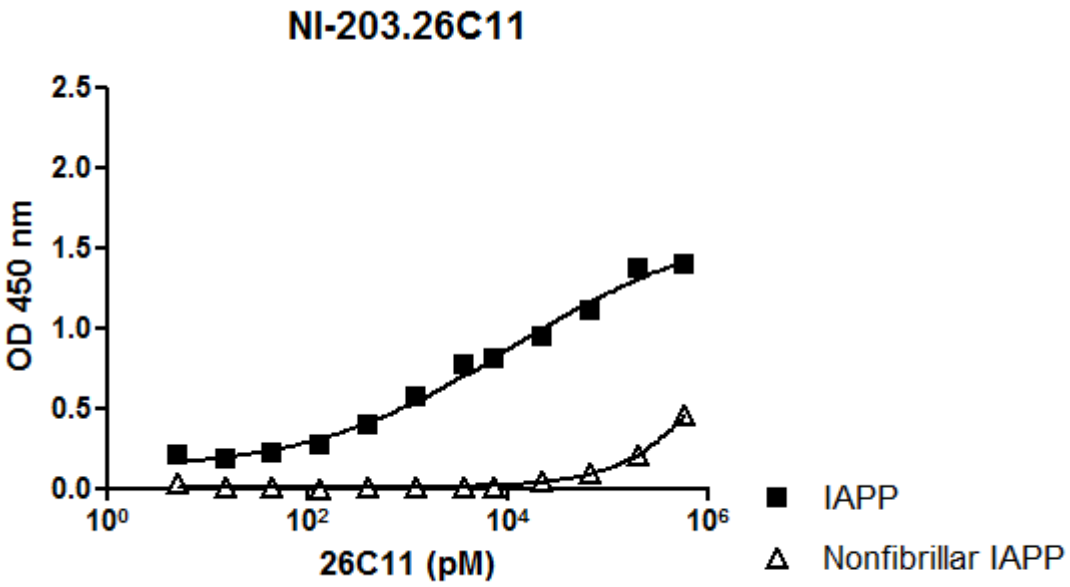

Fig 10: Plates were incubated with the indicated concentrations of recombinant human-derived NI-203.26C11 antibody. NI-203.26C11 binds with high affinity to IAPP aggregates (IAPP solution, 10 µg/ml) and with absence of binding to non-aggregated IAPP (10 µg/ml). Measurements were made in duplicate and background signal on BSA was subtracted. Data are expressed as mean optical density values at 450 nm (Data from Neurimmune).

These findings suggest that NI-203.26C11 antibody binds a conformational epitope exposed on aggregated IAPP species, but not to linear epitopes present in monomeric human IAPP molecules.

Finally, to avoid a mouse anti-human antibody response, chimeric antibodies consisting of human variable domains and murine constant regions were generated by protein engineering. Chimeric

antibodies were recombinantly produced in CHO cells for further *in vitro* characterization and for *in vivo* validation studies in transgenic mice. Endotoxin-free antibodies for in vivo validation were additionally purified by affinity chromatography.

4c. Intraperitoneal Glucose Tolerance Test (ipGTT)

The ipGTT protocol has been previously described by Ehses et al. (2010). After 12 hours fasting during the dark phase, mice were put in a restrainer for blood sampling. The most distal part of the tail was cut with a scalpel blade and blood was collected. Basal glycaemia and insulinemia were measured. Animals were weighted and received an i.p. injection of 20% glucose (2g/kg, 10ml/kg). Blood glucose and insulin levels were measured 15, 30, 60, 120 and 240 min after glucose injection. Glycemia was assessed using glucose strips and a glucometer (Breeze 2, Bayer, Mijdrecht, The Netherlands). The mean of two measurements was taken at every time point. If the measures differed by > 2mmol, a third measurement was taken. When glucose levels were above the measurement threshold of the glucometer (33.3 mmol/l), 3µl of blood were diluted 1:1 with 3µl NaCl (v/v). For insulin measurements, 25 µl of blood were collected using a heparinized capillary. Blood was transferred into a 500 µl Eppendorf tube containing EDTA (1/10; 50mM EDTA in 0.9% NaCl) on ice. Tubes were centrifuged for 5 minutes at 10'000 rpm. Plasma (10 µl) was transferred to a 96 well plate and stored at -20°C, for later analysis.

5. Insulin

Insulin plasma level was assessed with a mouse Insulin ELISA Kit from Mercodia (Uppsala, Sweden), following the manufacturer's instructions. The optical density was read at 450 nm with a Multiskan ELISA reader device (Thermo Labsystems, Milford, USA) and the different concentrations were calculated using cubic spline regression with the Ascent Software v.2.6 (Thermo scientific, Waltham, USA). In order to have reference values of untreated wild type mice, insulin levels of three 12 weeks old C57Bl/6 male mice were measured during an ipGTT.

6. Pancreas sampling and histology

After undergoing the third ipGTT at 3 months of age, mice were anesthetized with an i.p. injection of pentobarbital (40 mg/kg) and sacrificed by removing the blood from the caudal cave vein. The pancreas was collected and fixed with 4% paraformaldehyde (PFA) solution for 24 hours at room temperature. The tissues were embedded in paraffin blocks, cut with a microtome (Leica, Biosystems, Wetzlar, Germany) and mounted onto glass slides.

6a. Thioflavin-S staining

Thio-S staining was performed in order to detect the presence of amyloid fibrils. Thio-S binds to amyloid-fibrils but not to IAPP monomers. Thio-S is a benzothiazole dye that exhibits enhanced fluorescence upon binding to amyloid fibrils. The slides were heated at 65°C for one hour. They were incubated in the following series of solutions for deparaffinization and dehydration: two xylene washes (5 min each), followed by two 100% ethanol rinses (5 min each), followed by 95% ethanol, 70% ethanol, 50% ethanol, 30% ethanol, followed by H2O and a Tris-buffered saline solution with Tween 20 (TBST) wash for 5 min on a shaker. After deparaffinization, slices were stained for 15 minutes at room temperature (in the dark) with 1% Thio-S solution, differentiated in 96% ethanol and mounted with hydromount (National Diagnostics, Atlanta, USA) onto histological glass slides.

6b. Insulin staining

After deparaffinization, slices were immerged in 3% H2O2-methanol for 10min at room temperature to block endogenous peroxidase, rinsed in water and immerged in a solution containing 5% of normal goat serum, 5% of normal horse serum and 4% of BSA for 1 hour at room temperature as a serum blocking in order to reduce background staining. Primary antibodies were added at a dilution 1:3 (Polyclonal GP α Insulin, Dako, Baar, CH) for 4 hours at room temperature. After rinsing in water, the slides were incubated with secondary antibodies (Donkey α GP, Jackson Biotechnology, St Harbor, USA) at a dilution of 1:500 for 1 hour at room temperature. After another rinsing with water the slices were incubated for 30 minutes at room temperature with Vectastain ABC reagent (PK-600 Standard, Vector Laboratories, Burlingame, USA). The slides were rinsed again with water and incubated for about 7 minutes with DAB reagent (3,3'-diaminobenzidine tetrahydrochloride, Thermo Scientific, Waltham, USA) at a dilution of 1:10, at room temperature. The reaction was stopped with water. The slides were then incubated for 1-3 minutes in Couterstain Hem alum solution (Roth, Zurich, CH). After dehydration, the slices were mounted with mounting medium (Eukitt, Sigma Aldrich, St Louis, USA).

7. Statistics

All statistics were performed using the software Graphpad Prism 5 (San Diego, USA). One-way analysis of variances (ANOVA) and Tukey test for post hoc test were used. A p value <0.05 was considered statistically significant.

Results

1. Animals

Homozygous mice developed diabetes between 10 and 12 weeks of age. Fasting hyperglycaemia, glucose intolerance and impaired insulin secretion were observed in both the homozygous-PBS (homo-PBS) and homozygous-antibody (homo-AB) group (see Fig. 2, 4, 5, 6 and 7). Some mice died spontaneously between 10 and 12 weeks of age in both homozygous groups, presumably following complications due to their severe diabetic phenotype. The final number of animals was 12 mice in the homo-PBS and 13 mice in the homo-AB group. Hemizygous mice (n=10) did not develop a diabetic phenotype at any time during the course of the study.

2. Body weight

Baseline body weight was determined at 4 weeks of age, before mice were randomly assigned to their respective groups and showed no significant difference among the groups. After 4 weeks from the beginning of the immunization protocol, i.e. at an age of approximately 8 weeks, both homo-PBS and homo-AB showed lower body weight in comparison to the hemi-PBS control group. At this time point, mean body weight of the homo-PBS and the homo-AB mice was about 8% less than that of the hemi-PBS mice. However, no difference in body weight was observed between the homo-PBS and the homo-AB group at any time point; suggesting no influence of the anti-hIAPP antibody treatment on body weight gain in this mouse strain.

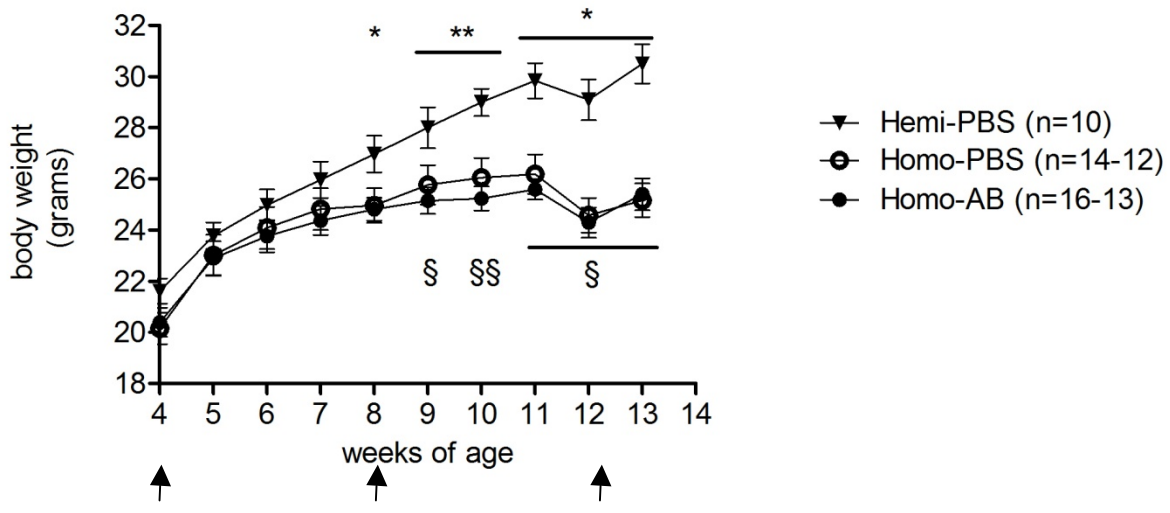

Fig 11: Body weight in hemi-PBS, homo-PBS and homo-AB mice from 4 to 13 weeks of age. Treatment with either PBS or anti-hIAPP antibodies was started at 4 weeks of age (§=p<0.05, §§=p<0.01 between the hemi-PBS and the homo-PBS group, *=p<0.05, **=p<0.01 between the hemi-PBS and the homo-AB group. Arrows indicate the time when ipGTTs were performed. Values are shown as means ± SE.

3. Fasting blood glucose levels

At one month of age, mean fasting blood glucose levels in the homo-PBS group were slightly but significantly higher than in the hemi-PBS group (9.0 ± 0.8 mmol/l and 6.1 ± 0.4 mmol/l, respectively, $p<0.05$). At the same time point, fasting glucose concentration in the homo-AB group (8.3 ± 0.9 mmol/l) was not significantly different from either the hemi-PBS or the homo-PBS group.
At two months of age, a tendency for higher fasting glucose levels was observed in the homo-PBS group (12.3 ± 2.5 mmol/l) compared to the hemi-PBS group (6.0 ± 0.4 mmol/l), though the difference was not statistically significant. Fasting glycaemia in the homo-AB group was significantly higher (17.4 ± 3.3 mmol/l) in comparison with the hemi-PBS group but did not differ from the levels in the homo-PBS mice.

After three months of age, fasting glucose levels in the homo-PBS and homo-AB mice were about 2-2.5 times higher than values measured at one month of age. However, blood glucose levels in the hemi-PBS were significantly different only compared to the homo-AB group but not to the homo-PBS group; this may have been due to the large variability within the homo-PBS group. Fasting blood glucose values in the homo-PBS group and the homo-AB group did not differ at any time point (Fig.12).

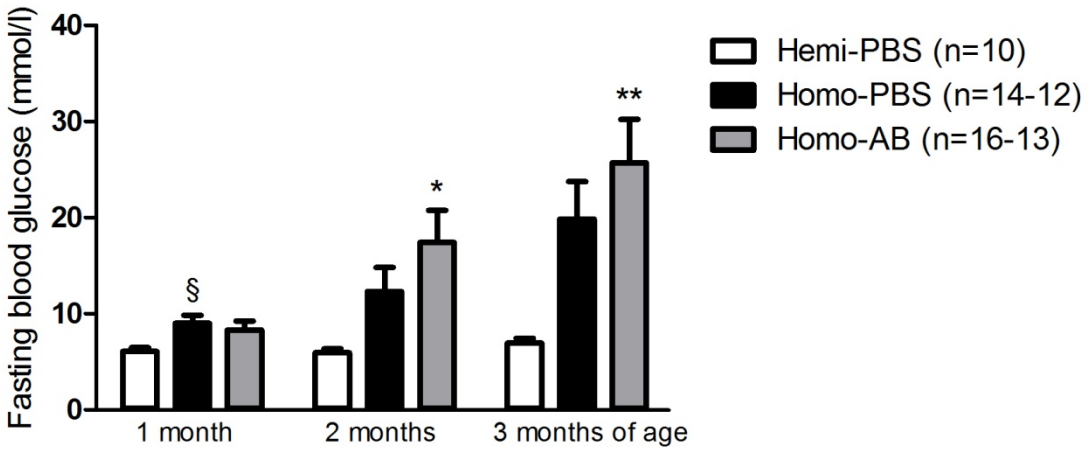

Fig 12: Fasting blood glucose level (after 12h fasting), in hemi-PBS, homo-PBS and homo-AB group, at one, two and three months of age. ANOVA showed a significant increase in the fasting blood glucose level in homo-PBS compared to hemi-PBS mice at one month of age (§=$p<0.05$). A significant increase of fasting blood glucose in the homo-AB compared to the hemi-PBS group was observed at two and three months of age (*=$p<0.05$, **=$p<0.01$). The values are shown as mean ± SE.

4. Fasting insulin levels

At one month of age, fasting insulin levels in the hemi-PBS group (0.61 ± 0.1 µg/l) were similar to the levels measured in the homo-PBS (0.51 ± 0.1 µg/l) and homo-AB (0.60 ± 0.04 µg/l).

At two months of age, insulin concentrations in homo-PBS (0.27 ± 0.10 µg/l) and homo-AB mice (0.36 ± 0.10 µg/l) were similar and did not significantly differ from the hemi-PBS group (0.39 ± 0.10 µg/l). However, in all three groups of mice, insulin levels tended to decrease in comparison with the values measured at one month of age.

At three months of age, a tendency for lower fasting insulin levels in the homo-PBS (0.30 ± 0.09 µg/l) and homo-AB (0.21 ± 0.06 µg/l) groups in comparison with the hemi-PBS (0.50 ± 0.1 µg/l) group was observed, however, it did not reach statistically significance. The homo-AB group showed a significant decrease in fasting insulin concentration between the first and the third month of age ($P<0.01$).

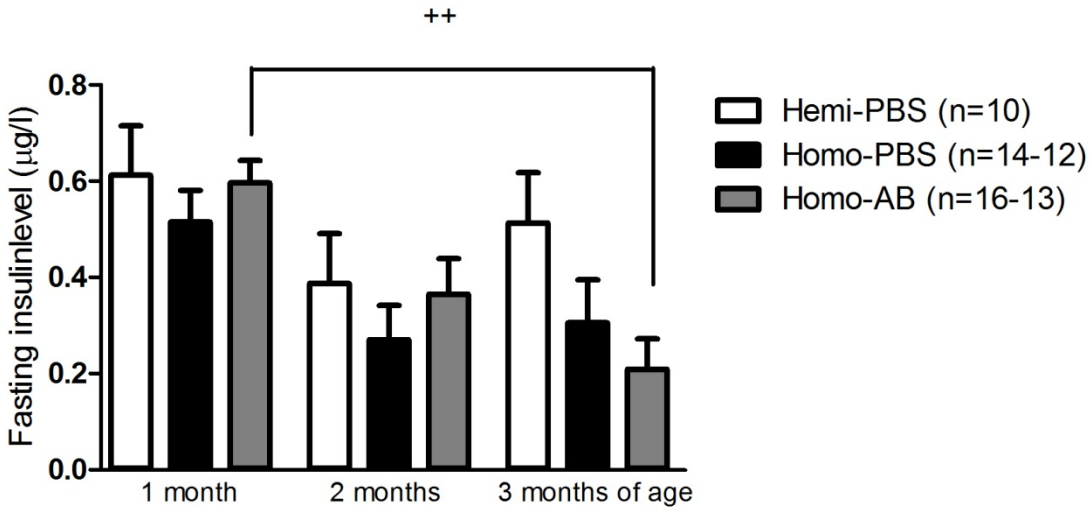

Fig.13: Fasting insulin levels (after 12h fasting) at one, two and three month of age in the hemi-PBS, homo-PBS and homo-AB group. No statistically significant differences were observed between the groups at any time point. The homo-AB group showed a significant decrease in fasting insulin levels between one and three months of age (++ =$p<0.01$).

5. Glycaemia during ipGTT

During the first ipGTT conducted at one month of age, i.e. before any treatment was started, baseline glycaemia was significantly elevated in the homo-PBS group in comparison with the hemi-PBS group ($p<0.05$). Plasma glucose levels were significantly higher at 30 ($p<0.01$) and 60 ($p<0.01$) minutes in both homo-PBS and homo-AB groups compared with the hemi-PBS group (see Fig.14).

However, glucose areas under the curve (AUC) above the respective baseline were similar in all groups (see Fig.17).

At two months of age, i.e. four weeks after the first treatment, baseline glycaemia tended to be higher in the homo-PBS group compared to the hemi-PBS group and was significantly higher in the homo-AB group compared to the hemi-PBS group ($p<0.05$, see Fig. 15). Glucose concentrations in the homozygous groups were significantly higher at 30 and 60 minutes compared to the values observed in the hemi-PBS group ($p<0.01$ at both time points). In the homo-AB group, glycaemia remained significantly higher until 120 minutes after glucose injection ($p<0.05$). The AUC of both homo-PBS and homo-AB groups were higher compared to AUC of the hemi-PBS group, even though the difference was not significant. AUCs were not significantly different between the homo-PBS and the homo-AB group (see Fig. 17).

At three months of age, baseline glycaemia was higher in the homo-PBS and significantly increased in the homo-AB group ($p<0.01$) in comparison with the hemi-PBS group. Glycaemia was significantly higher from 15 to 120 minutes after glucose injection in both homo-PBS and homo-AB group compared with hemi-PBS group (see Fig. 16). However, there were no differences in the AUCs above baseline among the groups (see Fig. 17).

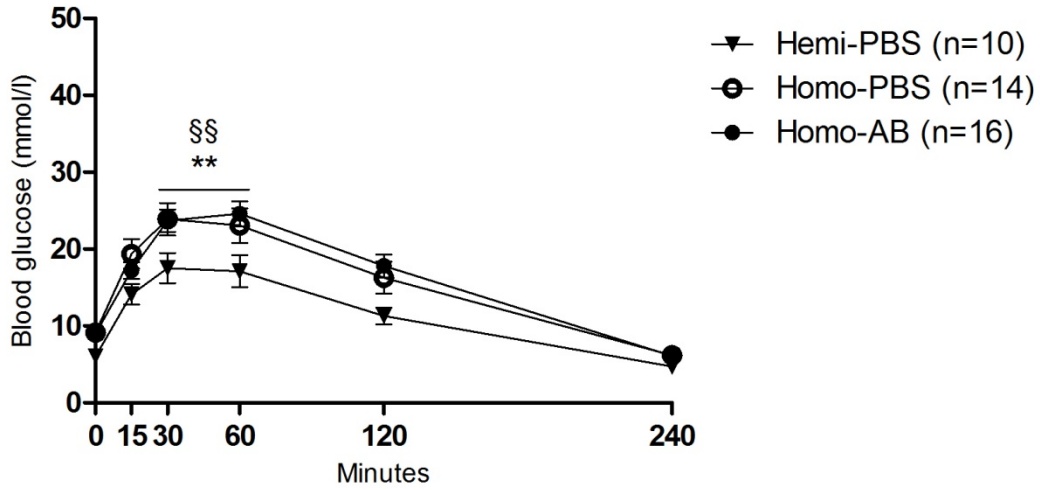

Fig. 14: Glycaemia during ipGTT in one-month old mice. ANOVA showed a significant increase in glycaemia at 30 and 60 minutes after glucose injection in both homo-AB and homo-PBS (**=$p<0.01$, §§=$p<0.01$, respectively) versus hemi-PBS mice. The values are shown as mean ± SE.

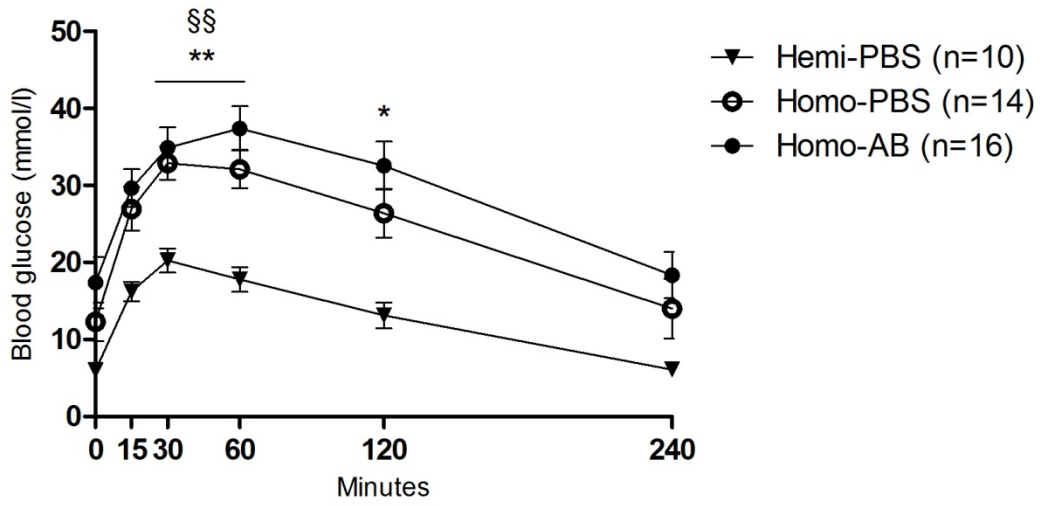

Fig. 15: Glycaemia during ipGTT in two-month old mice. ANOVA showed a significant increase in glycaemia at 30 and 60 and 120 minutes after glucose injection in both homo-AB and homo-PBS (* p<0.05, **=p<0.01, §§ p<0.01, respectively) compared with hemi-PBS group. There is no significant difference between the groups at baseline. Values are shown as means ± SE.

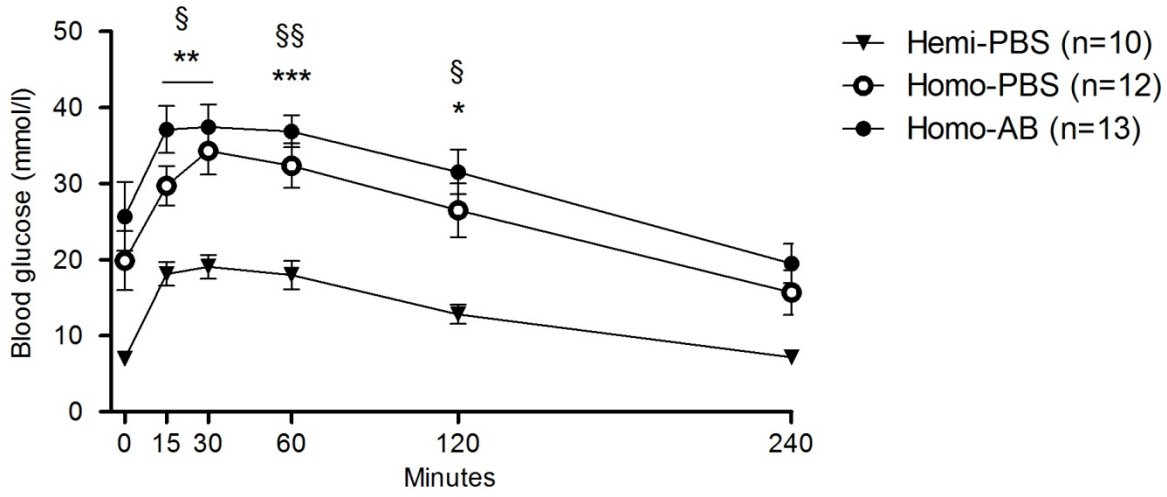

Fig. 16: Glycaemia during ipGTT in three-month old mice. ANOVA showed a significant increase in glycaemia at 15, 30, 60, and 120 minutes after glucose injection in both homo-AB and homo-PBS (* =p<0.05, **= p<0.01, *** =p<0.001, §= p<0.05, §§ =p<0.01, respectively), in comparison with the hemi-PBS group. There is no significant difference between the groups at baseline Values are shown as mean ± SE.

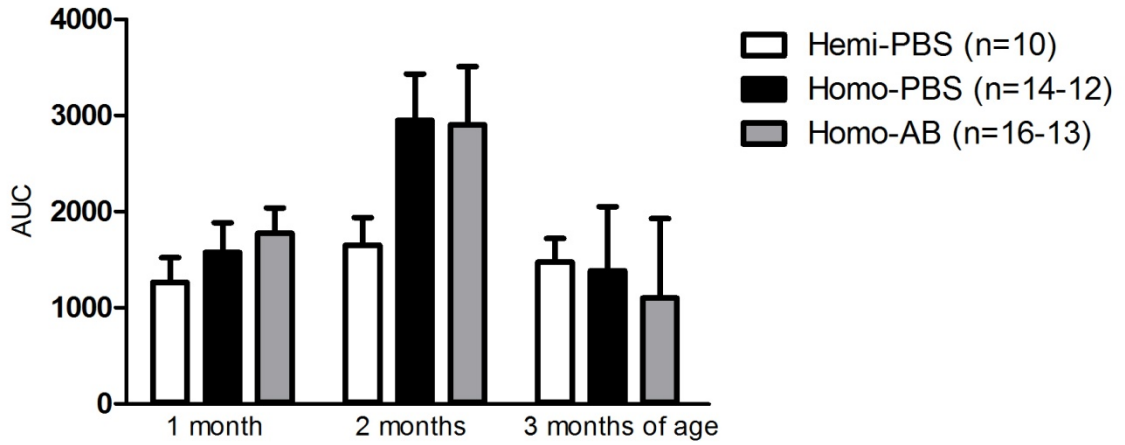

Fig. 17: Area under the curve of glycaemia (blood glucose in mmol/l/240 minutes) above respective baseline levels during ipGTTs in hemi-PBS, homo-PBS and homo-AB, at one, two and three months of age. Values are shown as mean ± SE.

6. Insulinemia during ipGTT

Unexpectedly, plasma insulin levels did not increase after glucose injection in any of the groups. At one month of age, glucose-stimulated insulin response in the hemi-PBS group showed a small increase 15 minutes after glucose injection and seemed to be higher at all time points as compared to both homozygous groups. Nevertheless, the difference was significant only at 60 minutes. Insulin levels were similar in both homo-PBS and homo-AB groups at all time points (Fig.18).

At two months of age, the hemi-PBS group showed a similar pattern of insulin response to glucose as shown at one month of age, though, mean insulin levels were lower. Plasma insulin concentration in the hemi-PBS group was higher from 30 to 120 minutes after glucose injection as compared to both homozygous groups (Fig.19).

At three months of age, the insulin concentration during the ipGTT was similar among the three groups except that at 120 minutes, when both homozygous groups had lower insulin levels compared to the hemi-PBS group (Fig.20). When data were examined as change over time, mean insulin levels seemed to decrease over time in all groups.

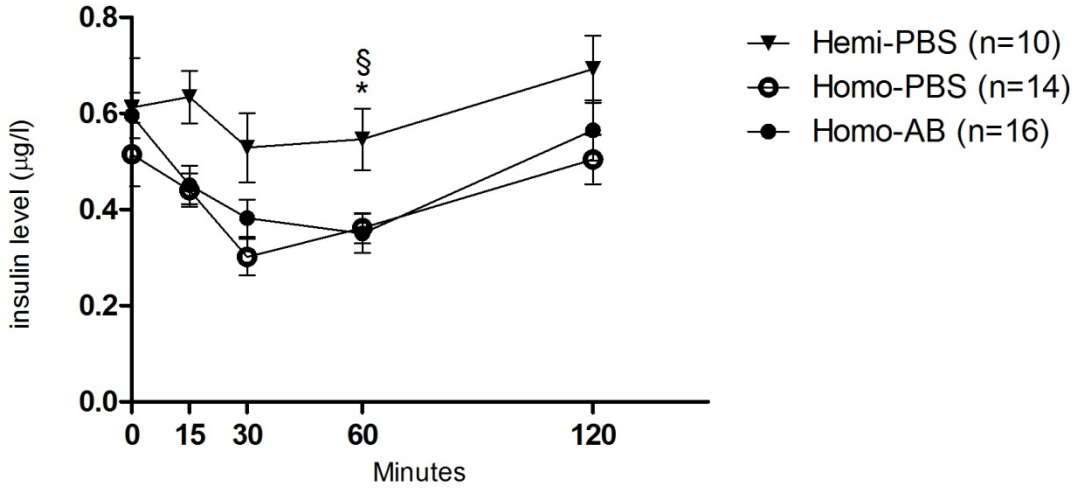

Fig. 18: Insulinemia during ipGTT in one month old mice. ANOVA showed a significant decrease in insulin levels in both homo-PBS and homo-AB group compared to the hemi-PBS group at 60 minutes after glucose injection (§= $p<0.05$, * =$p<0.05$, respectively). Values are shown as means ± SE.

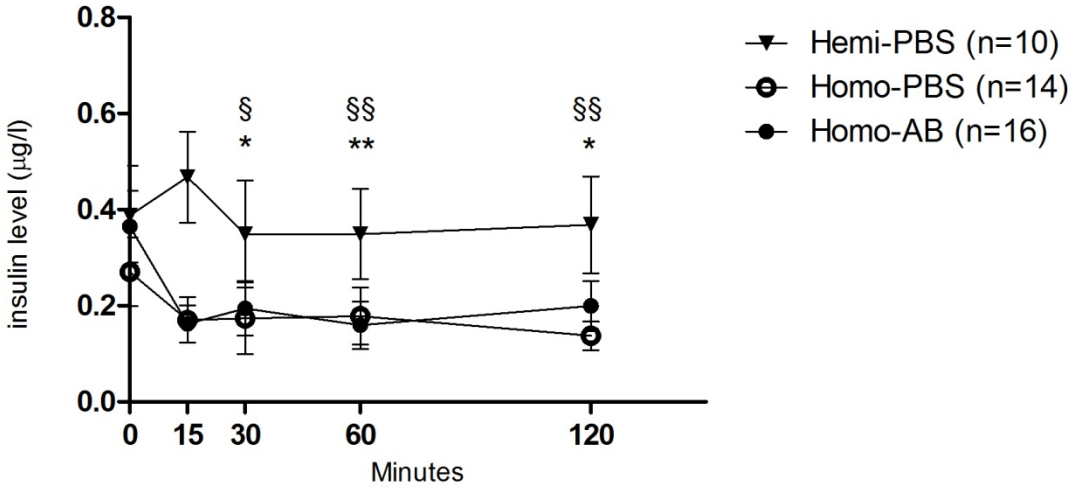

Fig. 19: Insulinemia during ipGTT in two-month old mice. The values are shown as means ± SE. ANOVA showed a significant decrease in insulin levels in homo-PBS and homo-AB group in comparison with the hemi-PBS group, at 30, 60 and 120 minutes after glucose injection (§ $p<0.05$, §§ =$p<0.01$,*= $p<0.05$, ** =$p<0.01$, respectively).

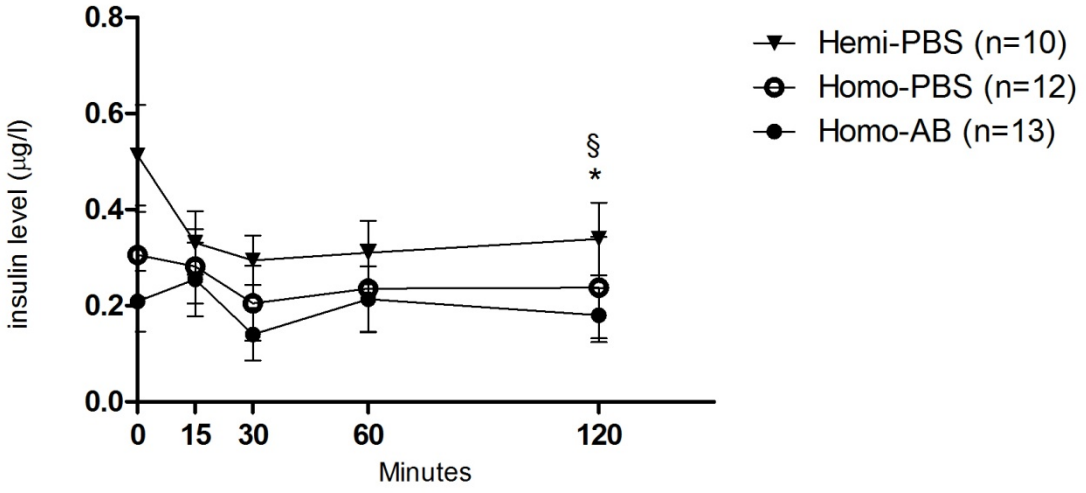

Fig. 20: Insulinemia during ipGTT in three-month old mice. The values are shown as means ± SE. ANOVA showed a significant decrease in insulin level in both homo-PBS and homo-AB group in comparison with the hemi-PBS group at 120 minutes after glucose injection (§ =$p<0.05$, * =$p<0.05$, respectively).

The glucose-induced changes in plasma insulin were unexpected in all three groups of mice, meaning that insulin levels decreased rather than increased after glucose injection. For comparison purposes, an ipGTT was performed in a group of untreated 12 weeks old C57Bl/6 male mice (n=3), from which published references values on insulin levels during ipGTTs are available (K. Kaku et al., 1998). In these mice, insulin peaked 15 minutes after glucose injection and then decreased to levels lower than baseline (see Fig. 21); thus, mimicking the insulin response to glucose reported in the literature (K. Kaku et al., 1998). Nonetheless, the insulin response was relatively small but the AUC of insulin was positive, while the calculated AUCs above respective baselines of the hemi-PBS, homo-PBS and homo-AB at one, two and three months of ages were all negative (Fig. 22).

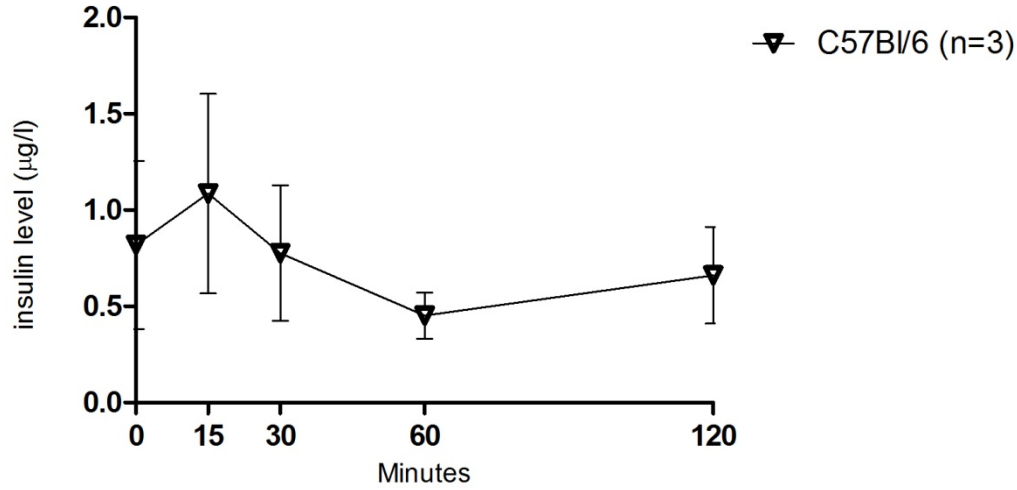

Fig. 21: Insulinemia during ipGTT in three C57BL/6 mice. Values are shown as mean ± SE.

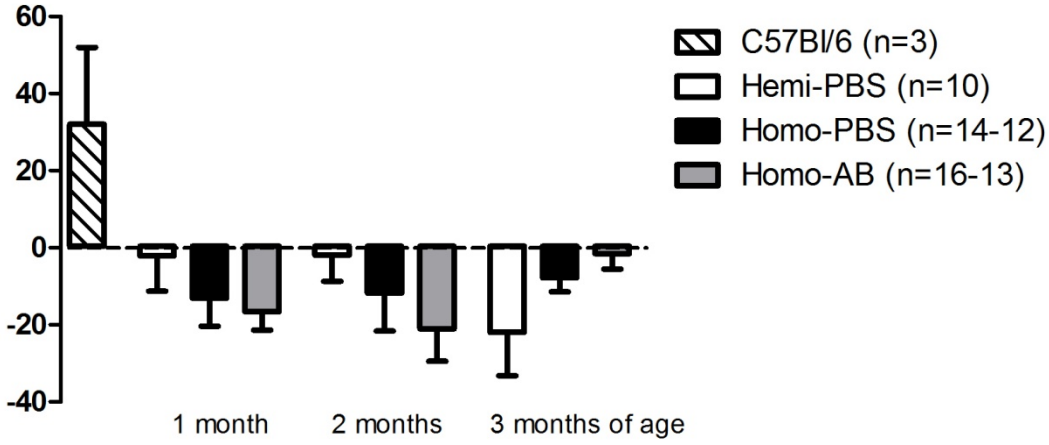

Fig 22: Area under the curve of the plasma insulin (µg/l/120minutes) level during ipGTT in C57Bl/6 control mice (n=3) compared to the AUCs of the hemi-PBS, homo-PBS and homo-AB group. Values are shown as mean ± SE and are expressed relative to the respective baselines.

7. Thioflavin-S staining of pancreas

At the end of the study, the mice were euthanized and the pancreas collected for histological analysis. Thio-S staining was performed to detect the presence of amyloid deposits in the pancreas of the experimental mice. According to the literature (M. Couce et al, 1996; J. Janson et al., 1996), Thio-S-positive extracellular amyloid deposition should not be present in hemizygous mice while it should be visible under electron microscopy in homozygous mice (R.L. Hull et al., 2005). Pancreas sections from hemizygous animals were therefore used as a negative control.

As shown in Fig. 23, extracellular amyloid deposits were not detected in the pancreas of both homozygous groups. As positive control, pancreata from 4.5 months old heterozygous mice with a different background, (FVB(h-IAPP)xDBA/2J), fed with high fat diet, were used. In previous studies (R.L. Hull et al., 2005), this model showed visible extracellular amyloid deposition under light microscopy. The DBA/2J background is believed to be determinant for the magnitude of islet amyloid formation, although the mechanism is not yet completely clear. It is believed that an increased susceptibility to dietary fat-related changes and an increased insulin release may play a role for the extent of the extracellular deposition. Fig. 24 shows Thio-S-positive staining in the pancreas section of a FVB(h-IAPP)xDBA/2J control mouse.

A.

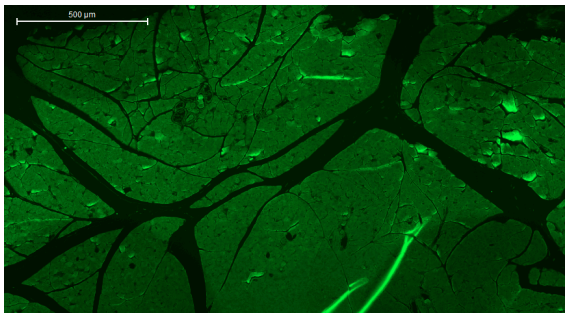

B.

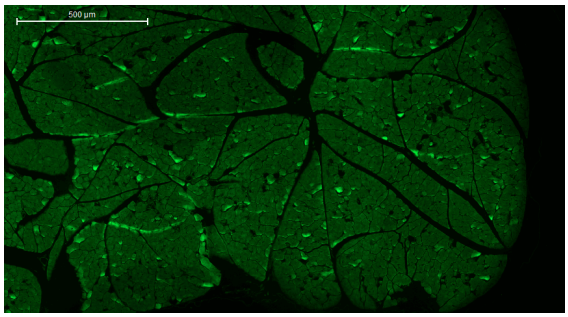

C.

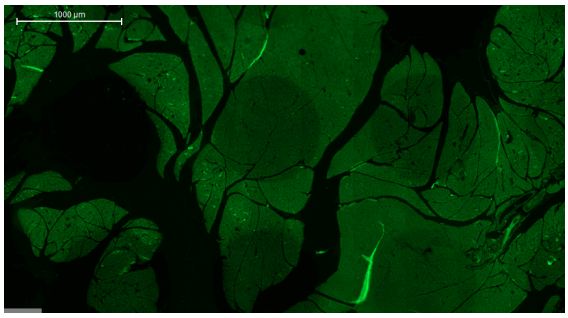

Fig.23: Light microscope pictures of Thio-S- positive staining in pancreas sections from homo-PBS, homo-AB and hemi-PBS. A. Homo-AB group; B. Homo-PBS group; C. Hemi-PBS group. Amyloid deposition was not observed in any of the groups.

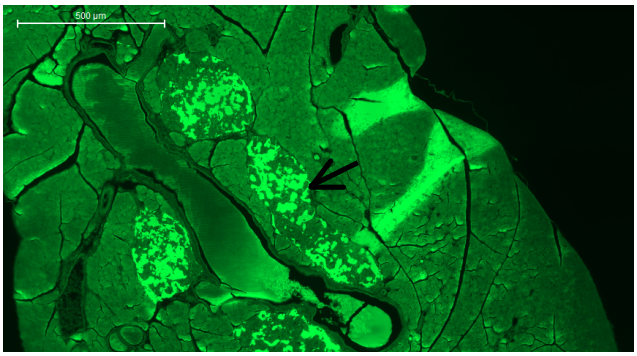

Fig. 24: Light microscope pictures of Thio-S-positive staining in pancreas sections from one heterozygous tg/- FVB(h-IAPP)xDBA/2J mouse at 4.5 months of age. Amyloid deposition was clearly visible in large parts of the islets (arrow).

8. Insulin staining of pancreas

Insulin staining showed a reduction in the average size of islets in both homozygous groups. Only a few insulin-positive cells could be observed in the islets of those groups, (Fig. 26 and 27). In comparison, islets in the pancreas of the hemizygous group (Fig. 25) seemed to be bigger in size and to contain more insulin-positive stained β-cells compared to both homozygous groups. However, no quantitative analysis of insulin-positive stained areas was conducted.

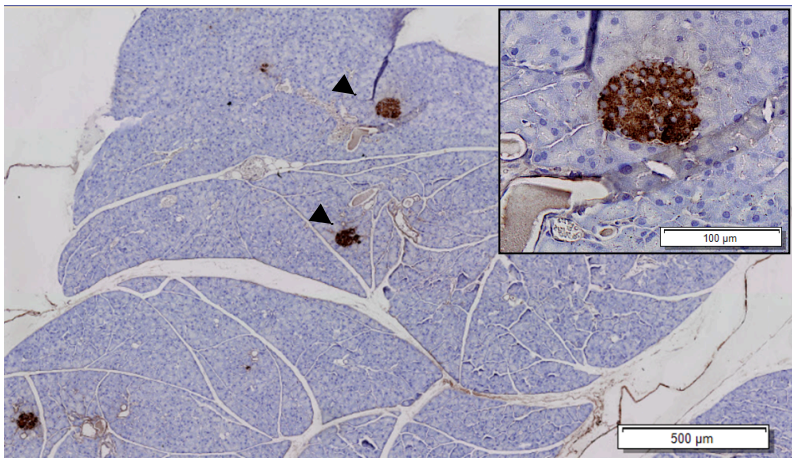

Fig. 25: Insulin staining (brown) in pancreas sections of hemizygous-PBS mice. The size and the number of the insulin-positive stained islets (arrow) appeared to be normal.

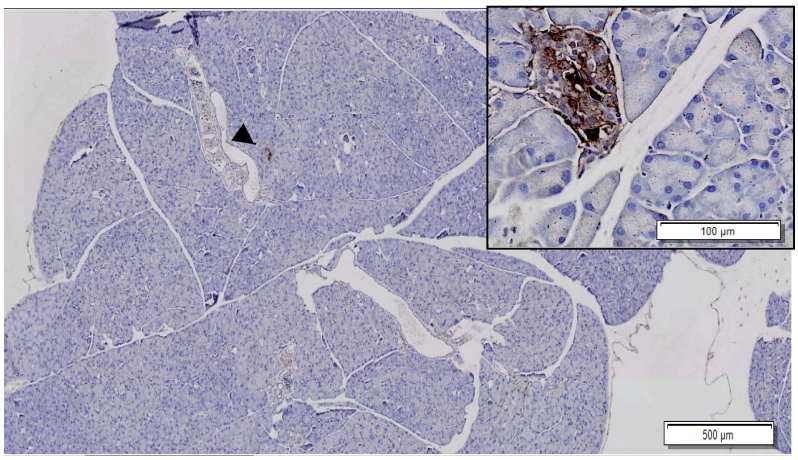

Fig. 26: Insulin staining (brown) in pancreas sections of homo-AB mice. Due to the loss of insulin stained β-cells, the size of islets (arrow) appeared to be smaller in comparison with insulin stained areas in the pancreas of hemizygous mice of the same age (see Fig 25)

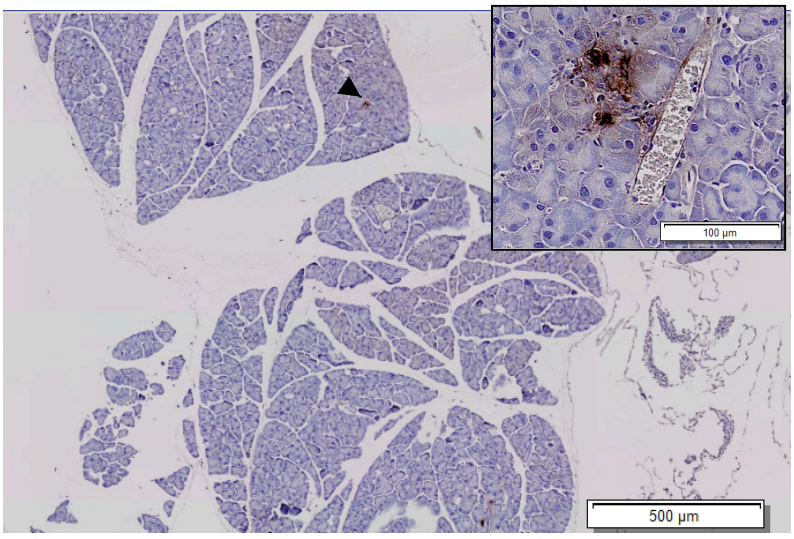

Fig 27: Insulin staining (brown) in pancreas sections of homo-PBS mice. As for the homo-AB group, insulin-positive islet areas are strikingly smaller than in heterozygous mice of the same age (see Fig 25).

Discussion

The aim of the present study was to test the therapeutic efficacy of a novel therapy for type-2 diabetes mellitus based on high affinity human derived antibodies targeting pathologically misfolded forms of human islet amyloid polypeptide (hIAPP) in a transgenic mouse model of T2DM expressing hIAPP.

IAPP is a peptide hormone co-secreted with insulin by pancreatic β-cells. In T2DM, genetic determinants and environmental factors lead to the development of insulin resistance followed by a compensatory increase in β-cell mass and insulin and IAPP secretion to maintain normal blood glucose levels. The resulting high concentration of IAPP favours the formation of toxic IAPP oligomers and eventually the deposition of IAPP fibrils which is found in more than 90% of T2DM patients. The deposition of IAPP correlates with the reduction in insulin producing β-cells (A. Clark and M.R. Nilsson, 2004).

Our immunotherapeutic approach was based on the identification, characterization and recombinant production of human-derived monoclonal antibodies specific for toxic hIAPP aggregates from pools of healthy donors or donors with mild forms or unusually slow progressing courses of T2DM. Whereas most antibody-based therapeutic approaches focus on humanized molecules, the method described in this thesis had the principal advantage of a superior safety profile when compared with engineered antibodies or antibodies isolated from non human-sources. Lead antibody candidates were validated *in vitro* for their affinity and selectivity to pathological hIAPP in pancreatic tissue of human diabetic subjects. The NI 203.26C11 antibody showed high affinity for pathological hIAPP and no binding to the native conformation of physiological monomeric hIAPP in healthy subjects. Thus, NI 203.26C11 was selected for validation *in vivo* in transgenic mice expressing hIAPP.

IAPP in mice and rats shares a large degree of homology with human IAPP but differs from human IAPP by substitution of proline residues in the amyloidogenic portion of IAPP. Therefore, mouse and rat IAPP does not form amyloid tendrils or oligomers nor do mice or rats spontaneously develop diabetes in midlife. Thus, in order to study the diabetogenic role of hIAPP in mice, rodent model transgenic for hIAPP were developed.

In the present study, the therapeutic efficacy of the NI 203.26C11 antibody in clearing existing hIAPP deposits and in preventing further build-up was studied in FVB/N-Tg(Ins2-IAPP)RHFSoel/J mice (RIPHAT mice). The RIPHAT mice express hIAPP under the regulatory control of the rat insulin II promoter. While hemizygous mice show no symptoms of spontaneous disease, homozygous males spontaneously develop diabetes mellitus due to β-cell death, associated with impaired insulin

secretion (hypoinsulinemia), hyperglycemia, and abnormal intracellular aggregates of hIAPP. For this study, male homozygous mice were used because females showed a more subtle phenotype with slower progression or absence of diabetes (J. Janson et al., 1996). Mice were fed *ad libitum* with a conventional chow diet, in order to minimize any confounding effect due to peripheral insulin resistance induced by dietary fat overload.

Consistent with the literature (M. Couce et al,, 1996), hemizygous control mice treated with PBS (hemi-PBS) did not develop diabetes mellitus and showed no changes in fasting blood glucose level and glucose tolerance over the whole experimental time.

Further, homozygous mice treated with PBS (homo-PBS) showed significantly higher glycaemia and impaired glucose tolerance compared to the hemi-PBS group from one month of age. The treatment with the NI 203-26C11 antibody did not improve fasting glycaemia or glucose tolerance in homo-AB mice compared to the homo-PBS. In fact, both groups of homozygous mice, independently from treatment allocation, developed a diabetic phenotype in comparison to the hemi-PBS mice.

A potential explanation for the lack of effect of the NI 203.26C11 antibody on basal glycemia might be that the twelve hours fasting period lowered blood glucose level to a level that prevented us from observing any difference between the homozygous groups. Nevertheless, both homozygous groups showed severe glucose intolerance already at the first ipGTT, which worsened with time, in comparison with the hemi-PBS group. In fact, blood glucose levels during the first 15-30 min of the second and third ipGTT were even higher than the upper detection limit of the glucometer (33 mmol/l). In such cases, an estimate of blood glycemia was obtained by diluting blood with saline (1:1). However, this dilution procedure revealed to be imprecise because no consistent values were obtained after linear dilution. Nonetheless, to the best of our knowledge, there are currently no comparable commercially available devices that could measure glycemia above 33 mmol/l in mice. To overcome this problem, glucose levels could have been measured in plasma by the hexokinase/glucose-6-phosphate dehydrogenase reaction. In this case, however, larger volumes of blood would have been required at each time point thus allowing less frequent samplings.

Insulin levels were significantly lower in the two homozygous groups in comparison with the hemi-PBS group. This finding was expected considering the glucose intolerance and the low number of insulin-positive cells which were observed in the homozygous mice. However, insulin levels were unexpectedly low also in the hemi-PBS group. In this group, glucose-induced increases of insulin reached a peak 15 min after glucose injection, but the peak was only observed during the first and second ipGTT.

Plasma levels of insulin have never been measured during ipGTT in this mouse strain. In the literature, glucose tolerance of the RIPHAT mice has always been tested with oral glucose tolerance tests. The oral administration of glucose in glucose tolerance tests triggers higher insulin secretion compared to ipGTTs, because oral glucose activates the secretion of endogenous incretins like GLP-1 and GIP (S. Andrikopoulos et al., 2008). Because in this study, glucose was administered intraperitoneally during the tolerance tests, glucose-induced insulin secretion was not augmented by incretin effects. We presumed that as a result, insulin levels were in many cases lower than the detection limit (0.025µg/l) of the ELISA assay and therefore could not be measured accurately.

In the literature, insulin levels in C57BL/6J mice during ipGTT are within the measurable ranges of typical ELISAs (K. Kaku et al., 1988). Therefore, in order to exclude any error of the technical execution of the ELISA, we performed an ipGTT in C57BL/6J mice and measured plasma insulin. As expected, plasma insulin in C57BL/6J mice was in the same range as reported in the literature (K. Kaku et al., 1988) suggesting that the very low insulin levels observed in the RIPHAT mice may be the result of considerably lower levels of systemic insulin in this strain.

Other conditions that may also have contributed to interfere with the measurement of plasma insulin is the presence of hemolysis in plasma samples, especially at the latest time point of the ipGTT. Hemolysis can interfere with the detection of insulin by the ELISA assay, as it is mentioned in manufacturer's instructions. Because the quantity of blood in multiple samples withdrawn is limited in mice, insulin levels were not measured in duplicates. Moreover, ipGTTs were performed after a twelve hours overnight fasting, which may have contributed to low insulin levels (S. Andrikopoulos et al., 2008).

In the literature (M. Couce et al., 1996), diabetes onset in the RIPHAT homozygous male mice is described between 4-8 weeks of age with spontaneous death around 16 weeks of age. The absence of consensual reference values of fasting glycemia and in glucose tolerance for a precise diagnosis of T2DM in mice prevented us from defining the exact time point of diabetes onset in the homozygous mice of our study. Furthermore, the total amount of water consumption and urine production was not measured. However, both homozygous groups presented with a polyuric and polydypsic phenotype already around two months of age (personal observations). In other studies conducted in mouse models for type 1 diabetes, animals with blood glucose concentrations equal to or over 300 mg/dl (which corresponds approximately to 16.7 mmol/l) were considered diabetic (M. Graham et al., 2011). According to these reference values, homo-AB and homo-PBS could have been considered diabetic at two and three months of age, respectively.

Thio-S positive extracellular amyloid load was not detected under light microscopy in neither of the experimental groups of mice. The lack of detectable Thio-S positive amyloid deposition in our study does not exclude the presence of small intracellular toxic oligomers. In fact, small intracellular hIAPP aggregations have been described in pancreas section from RIPHAT homozygous mice (J. Janson et al., 2006), however these observations were detected only through electron microscopy which was not available for our study.

We observed a decrease of the insulin-positive areas in sections of pancreata from both homozygous groups in comparison to the hemi-PBS group. This was accompanied by a reduction in the size of the islets in both homo-AB and homo-PBS groups. These observations indicate that the loss of β-cells might not be directly related to the presence of extracellular IAPP fibrils, but might be caused by other mechanisms. In fact, according to the literature, IAPP toxicity in the RIPHAT mice depends on the high IAPP intracellular concentration in the pancreas which in turn induces accumulation of polyubiquinated proteins ultimately leading to ER-stress. Moreover, the presence of non fibrillar IAPP formation may cause membrane damages, disruption of proteasome and be responsible for β-cell apoptosis, thus implying a direct cytotoxicity effect of soluble IAPP forms on β-cells (C.J. Huang et al., 2007). This may happen before extracellular amyloid can be detected with Thio-S staining.

The phenotype of the RIPHAT homozygous male was very severe and progressed rapidly in our study. Spontaneous death was observed during the experimental time in both homozygous groups. The NI 203.26C11 antibody administration did not show beneficial effects in preventing or slowing the progression of diabetes in this mouse strain. Nevertheless, the antibody administration was well tolerated and did not elicit any toxic or systemic immunoreaction. The normal progression of T2DM in humans is a chronic process that takes place over years (D.R. Whiting, 2011). Hence, it is difficult to predict the effect that a chronic anti-amyloid antibody administration would have in humans. The model used in our study presumably progressed too rapidly into a pathological phenotype which does not reflect the physiopathology of the disease in humans. Therefore, other animal model may be more appropriate to assess the efficiency of the antibodies and their potential contribution for the treatment of T2DM in humans.

In this regard, a study currently assesses the effect of the NI 203.26C11 antibody in hIAPP (hemizygous)/C57BL/6 x DBA mice. These mice do not develop spontaneous T2DM, but have impaired glucose tolerance during ipGTT due to decreased insulin secretion. They show extracellular amyloid deposition and evidence for decrease β- cell mass at about seven months of age (R.L. Hull et al., 2003; R.L. Hull et al., 2005; F. Wang et al., 2001). The slower progression of the disease in these mice makes them a more suitable model for the assessment of the therapeutic efficacy of human-

derived anti-hIAPP antibodies. Furthermore, the effect of the NI 203.26C11 antibody is currently under investigation in the so called RIPHAT rat model. RIPHAT rats present with a similar phenotype as the RIPHAT mice but with a much slower progression of T2DM (A.E. Butler et al., 2004).

Similar approaches of immunotherapy were developed for several brain diseases involving protein aggregation such as Alzheimer's disease, Parkinson's disease, and amyotrophic lateral sclerosis. The dosage (10mg/kg) of the NI 203.26C11 antibody administered in this study was based on Alzheimer's trials in which antibodies were required to cross the blood/brain barrier and reach the targeted brain areas. Targeting pancreatic islets via the systemic circulation may however more easily be achieved and may then require lower concentrations of antibody. Thus, it might then be that the antibody dosage used in the present study was too high and may have had neutralizing effect. Dose response studies will be needed to test this hypothesis.

In conclusion, administration of the human-derived IAPP-antibody NI 203.26C11 in RIPHAT mice was safe and well tolerated. However, the immunotherapy did not improve glucose control, glucose tolerance and insulin secretion nor was it effective in slowing the progression of diabetes in this mouse model transgenic for hIAPP. Under the experimental conditions of this study, we believe that the very rapid progression of islet degeneration in the transgenic mice may have prevented the beneficial effects of the immunotherapy. Nevertheless, preliminary results in other rodents models of T2DM showed that passive immunization with the IAPP-antibody NI 203.26C11 could ameliorate glucose control and insulin metabolism by targeting toxic aggregates of IAPP and reducing the loss of pancreatic β-cells.

Therefore, it may be concluded that the NI 203.26C11 antibody may represent a novel treatment for T2DM. However, further *in vivo* studies are required to test the therapeutic efficacy of this novel strategy for the treatment of T2DM.

References:

Andrikopoulos, S., et al. (2008). "Evaluating the glucose tolerance test in mice." Am J Physiol Endocrinol Metab **295**(6): E1323-1332.

Bagdade, J. D., et al. (1967). "The significance of basal insulin levels in the evaluation of the insulin response to glucose in diabetic and nondiabetic subjects." J Clin Invest **46**(10): 1549-1557.

Bard, F., et al. (2000). "Peripherally administered antibodies against amyloid beta-peptide enter the central nervous system and reduce pathology in a mouse model of Alzheimer disease." Nat Med **6**(8): 916-919.

Beard, J. C., et al. (1984). "Dexamethasone-induced insulin resistance enhances B cell responsiveness to glucose level in normal men." Am J Physiol **247**(5 Pt 1): E592-596.

Betsholtz, C., et al. (1989). "Islet amyloid polypeptide (IAPP):cDNA cloning and identification of an amyloidogenic region associated with the species-specific occurrence of age-related diabetes mellitus." Exp Cell Res **183**(2): 484-493.

Bordenave, S., et al. (2008). "Effects of acute exercise on insulin sensitivity, glucose effectiveness and disposition index in type 2 diabetic patients." Diabetes Metab **34**(3): 250-257.

Bryan, J., et al. (2005). "Insulin secretagogues, sulfonylurea receptors and K(ATP) channels." Curr Pharm Des **11**(21): 2699-2716.

Burks, D. J. and M. F. White (2001). "IRS proteins and beta-cell function." Diabetes **50 Suppl 1**: S140-145.

Bursch, W., et al. (2000). "Programmed cell death (PCD). Apoptosis, autophagic PCD, or others?" Ann N Y Acad Sci **926**: 1-12.

Butler, A. E., et al. (2004). "Diabetes due to a progressive defect in beta-cell mass in rats transgenic for human islet amyloid polypeptide (HIP Rat): a new model for type 2 diabetes." Diabetes **53**(6): 1509-1516.

Butler, A. E., et al. (2003). "Increased beta-cell apoptosis prevents adaptive increase in beta-cell mass in mouse model of type 2 diabetes: evidence for role of islet amyloid formation rather than direct action of amyloid." Diabetes **52**(9): 2304-2314.

Chen, M., et al. (1985). "Pathogenesis of age-related glucose intolerance in man: insulin resistance and decreased beta-cell function." J Clin Endocrinol Metab **60**(1): 13-20.

Christopoulos, G., et al. (1995). "Comparative distribution of receptors for amylin and the related peptides calcitonin gene related peptide and calcitonin in rat and monkey brain." Can J Physiol Pharmacol **73**(7): 1037-1041.

Clark, A. and M. R. Nilsson (2004). "Islet amyloid: a complication of islet dysfunction or an aetiological factor in Type 2 diabetes?" Diabetologia **47**(2): 157-169.

Clark, A., et al. (1988). "Islet amyloid, increased A-cells, reduced B-cells and exocrine fibrosis: quantitative changes in the pancreas in type 2 diabetes." Diabetes Res **9**(4): 151-159.

Clegg, D. J., et al. (2011). "Consumption of a high-fat diet induces central insulin resistance independent of adiposity." Physiol Behav **103**(1): 10-16.

Cnop, M., et al. (2002). "The concurrent accumulation of intra-abdominal and subcutaneous fat explains the association between insulin resistance and plasma leptin concentrations : distinct metabolic effects of two fat compartments." Diabetes **51**(4): 1005-1015.

Cohen, A. S. and E. Calkins (1959). "Electron microscopic observations on a fibrous component in amyloid of diverse origins." Nature **183**(4669): 1202-1203.

Conway, K. A., et al. (2003). "Emerging beta-amyloid therapies for the treatment of Alzheimer's disease." Curr Pharm Des **9**(6): 427-447.

Couce, M., et al. (1996). "Treatment with growth hormone and dexamethasone in mice transgenic for human islet amyloid polypeptide causes islet amyloidosis and beta-cell dysfunction." Diabetes **45**(8): 1094-1101.

Davenport, E. L., et al. (2008). "Untangling the unfolded protein response." Cell Cycle **7**(7): 865-869.

Davidson, H. W. and J. C. Hutton (1987). "The insulin-secretory-granule carboxypeptidase H. Purification and demonstration of involvement in proinsulin processing." Biochem J **245**(2): 575-582.

De Felice, F. G. and S. T. Ferreira (2002). "Beta-amyloid production, aggregation, and clearance as targets for therapy in Alzheimer's disease." Cell Mol Neurobiol **22**(5-6): 545-563.

de Koning, E. J., et al. (1993). "Diabetes mellitus in Macaca mulatta monkeys is characterised by islet amyloidosis and reduction in beta-cell population." Diabetologia **36**(5): 378-384.

de Koning, E. J., et al. (1994). "Human islet amyloid polypeptide accumulates at similar sites in islets of transgenic mice and humans." Diabetes **43**(5): 640-644.

Donath, M. Y. (2013). "Targeting inflammation in the treatment of type 2 diabetes." Diabetes Obes Metab **15 Suppl 3**: 193-196.

Donath, M. Y., et al. (1999). "Hyperglycemia-induced beta-cell apoptosis in pancreatic islets of Psammomys obesus during development of diabetes." Diabetes **48**(4): 738-744.

Donath, M. Y. and S. E. Shoelson (2011). "Type 2 diabetes as an inflammatory disease." Nat Rev Immunol **11**(2): 98-107.

Egert, S., et al. (2014). "Effects of an energy-restricted diet rich in plant-derived alpha-linolenic acid on systemic inflammation and endothelial function in overweight-to-obese patients with metabolic syndrome traits." Br J Nutr: 1-8.

Finegood, D. T., et al. (2001). "Beta-cell mass dynamics in Zucker diabetic fatty rats. Rosiglitazone prevents the rise in net cell death." Diabetes **50**(5): 1021-1029.

Fogar, P., et al. (1994). "Diabetes mellitus in pancreatic cancer follow-up." Anticancer Res **14**(6B): 2827-2830.

Games, D., et al. (1995). "Alzheimer-type neuropathology in transgenic mice overexpressing V717F beta-amyloid precursor protein." Nature **373**(6514): 523-527.

Games, D., et al. (2000). "Prevention and reduction of AD-type pathology in PDAPP mice immunized with A beta 1-42." Ann N Y Acad Sci **920**: 274-284.

Gill, A. M., et al. (1994). "Dexamethasone-induced hyperglycemia in obese Avy/a (viable yellow) female mice entails preferential induction of a hepatic estrogen sulfotransferase." Diabetes **43**(8): 999-1004.

Gleason, C. E., et al. (2000). "Determinants of glucose toxicity and its reversibility in the pancreatic islet beta-cell line, HIT-T15." Am J Physiol Endocrinol Metab **279**(5): E997-1002.

Goodpaster, B. H., et al. (1999). "Effects of weight loss on regional fat distribution and insulin sensitivity in obesity." Diabetes **48**(4): 839-847.

Graham, M. L., et al. (2011). "The streptozotocin-induced diabetic nude mouse model: differences between animals from different sources." Comp Med **61**(4): 356-360.

Guardado-Mendoza, R., et al. (2009). "Pancreatic islet amyloidosis, beta-cell apoptosis, and alpha-cell proliferation are determinants of islet remodeling in type-2 diabetic baboons." Proc Natl Acad Sci U S A **106**(33): 13992-13997.

Guariguata, L. (2012). "By the numbers: new estimates from the IDF Diabetes Atlas Update for 2012." Diabetes Res Clin Pract **98**(3): 524-525.

Gurlo, T., et al. (2010). "Evidence for proteotoxicity in beta cells in type 2 diabetes: toxic islet amyloid polypeptide oligomers form intracellularly in the secretory pathway." Am J Pathol **176**(2): 861-869.

Haass, C. and B. De Strooper (1999). "The presenilins in Alzheimer's disease--proteolysis holds the key." Science **286**(5441): 916-919.

Herndon, A. M., et al. (2014). "Oxidative modification, inflammation and amyloid in the normal and diabetic cat pancreas. " J Comp Pathol **151**(4) : 352-62.

Hock, C., et al. (2003). "Antibodies against beta-amyloid slow cognitive decline in Alzheimer's disease." Neuron **38**(4): 547-554.

Holscher, C. (2005). "Development of beta-amyloid-induced neurodegeneration in Alzheimer's disease and novel neuroprotective strategies." Rev Neurosci **16**(3): 181-212.

Hoppener, J. W., et al. (1999). "Extensive islet amyloid formation is induced by development of Type II diabetes mellitus and contributes to its progression: pathogenesis of diabetes in a mouse model." Diabetologia **42**(4): 427-434.

Hou, X., et al. (1999). "Prolonged exposure of pancreatic beta cells to raised glucose concentrations results in increased cellular content of islet amyloid polypeptide precursors." Diabetologia **42**(2): 188-194.

Howard, C. F., Jr. (1978). "Insular amyloidosis and diabetes mellitus in Macaca nigra." Diabetes **27**(4): 357-364.

Howard, C. F., Jr. (1986). "Longitudinal studies on the development of diabetes in individual Macaca nigra." Diabetologia **29**(5): 301-306.

Huang, C. J., et al. (2007). "Induction of endoplasmic reticulum stress-induced beta-cell apoptosis and accumulation of polyubiquitinated proteins by human islet amyloid polypeptide." Am J Physiol Endocrinol Metab **293**(6): E1656-1662.

Hull, R. L., et al. (2003). "Increased dietary fat promotes islet amyloid formation and beta-cell secretory dysfunction in a transgenic mouse model of islet amyloid." Diabetes **52**(2): 372-379.

Hull, R. L., et al. (2005). "Genetic background determines the extent of islet amyloid formation in human islet amyloid polypeptide transgenic mice." Am J Physiol Endocrinol Metab **289**(4): E703-709.

Ihara, Y., et al. (1999). "Hyperglycemia causes oxidative stress in pancreatic beta-cells of GK rats, a model of type 2 diabetes." Diabetes **48**(4): 927-932.

Jaikaran, E. T. and A. Clark (2001). "Islet amyloid and type 2 diabetes: from molecular misfolding to islet pathophysiology." Biochim Biophys Acta **1537**(3): 179-203.

Janson, J., et al. (2004). "Increased risk of type 2 diabetes in Alzheimer disease." Diabetes **53**(2): 474-481.

Janson, J., et al. (1996). "Spontaneous diabetes mellitus in transgenic mice expressing human islet amyloid polypeptide." Proc Natl Acad Sci U S A **93**(14): 7283-7288.

Jindal, H., et al. (2014). "Alzheimer disease immunotherapeutics: Then and now." Hum Vaccin Immunother **10**(9).

Johnson, K. H., et al. (1989). "Islet amyloid, islet-amyloid polypeptide, and diabetes mellitus." N Engl J Med **321**(8): 513-518.

Jonas, J. C., et al. (1999). "Chronic hyperglycemia triggers loss of pancreatic beta cell differentiation in an animal model of diabetes." J Biol Chem **274**(20): 14112-14121.

Kahn, S. E., et al. (1989). "Increased beta-cell secretory capacity as mechanism for islet adaptation to nicotinic acid-induced insulin resistance." Diabetes **38**(5): 562-568.

Kahn, S. E., et al. (1990). "Effect of exercise on insulin action, glucose tolerance, and insulin secretion in aging." Am J Physiol **258**(6 Pt 1): E937-943.

Kaku, K., et al. (1988). "Genetic analysis of glucose tolerance in inbred mouse strains. Evidence for polygenic control." Diabetes **37**(6): 707-713.

Kawahara, M., et al. (2000). "Alzheimer's beta-amyloid, human islet amylin, and prion protein fragment evoke intracellular free calcium elevations by a common mechanism in a hypothalamic GnRH neuronal cell line." J Biol Chem **275**(19): 14077-14083.

Kawasaki, F., et al. (2005). "Structural and functional analysis of pancreatic islets preserved by pioglitazone in db/db mice." Am J Physiol Endocrinol Metab **288**(3): E510-518.

Kido, Y., et al. (2001). "Clinical review 125: The insulin receptor and its cellular targets." J Clin Endocrinol Metab **86**(3): 972-979.

Lazarevic, G., et al. (2006). "A physical activity programme and its effects on insulin resistance and oxidative defense in obese male patients with type 2 diabetes mellitus." Diabetes Metab **32**(6): 583-590.

Lee, Y., et al. (1994). "Beta-cell lipotoxicity in the pathogenesis of non-insulin-dependent diabetes mellitus of obese rats: impairment in adipocyte-beta-cell relationships." Proc Natl Acad Sci U S A **91**(23): 10878-10882.

Li, L. and C. Holscher (2007). "Common pathological processes in Alzheimer disease and type 2 diabetes: a review." Brain Res Rev **56**(2): 384-402.

Lutz, T. A. (2006). "Amylinergic control of food intake." Physiol Behav **89**(4): 465-471.

Lutz, T. A. (2013). "The interaction of amylin with other hormones in the control of eating." Diabetes Obes Metab **15**(2): 99-111.

Lutz, T. A., et al. (1995). "Amylin decreases meal size in rats." Physiol Behav **58**(6): 1197-1202.

MacIntyre, I. (1989). "Amylinamide, bone conservation, and pancreatic beta cells." Lancet **2**(8670): 1026-1027.

Marciniak, S. J. and D. Ron (2006). "Endoplasmic reticulum stress signaling in disease." Physiol Rev **86**(4): 1133-1149.

Marciniuk, K., et al. (2013). "Evidence for prion-like mechanisms in several neurodegenerative diseases: potential implications for immunotherapy." Clin Dev Immunol **2013**: 473706.

Marzban, L., et al. (2004). "Role of beta-cell prohormone convertase (PC)1/3 in processing of pro-islet amyloid polypeptide." Diabetes **53**(1): 141-148.

Masliah, E., et al. (1996). "Comparison of neurodegenerative pathology in transgenic mice overexpressing V717F beta-amyloid precursor protein and Alzheimer's disease." J Neurosci **16**(18): 5795-5811.

Mason, J. M., et al. (2003). "Design strategies for anti-amyloid agents." Curr Opin Struct Biol **13**(4): 526-532.

Masters, S. L., et al. (2010). "Activation of the NLRP3 inflammasome by islet amyloid polypeptide provides a mechanism for enhanced IL-1beta in type 2 diabetes." Nat Immunol **11**(10): 897-904.

Matsuoka, T., et al. (1997). "Glycation-dependent, reactive oxygen species-mediated suppression of the insulin gene promoter activity in HIT cells." J Clin Invest **99**(1): 144-150.

Mohanty, S., et al. (2005). "Overexpression of IRS2 in isolated pancreatic islets causes proliferation and protects human beta-cells from hyperglycemia-induced apoptosis." Exp Cell Res **303**(1): 68-78.

Moriarty, D. F. and D. P. Raleigh (1999). "Effects of sequential proline substitutions on amyloid formation by human amylin20-29." Biochemistry **38**(6): 1811-1818.

Movassat, J., et al. (1997). "Impaired development of pancreatic beta-cell mass is a primary event during the progression to diabetes in the GK rat." Diabetologia **40**(8): 916-925.

Nandi, A., et al. (2004). "Mouse models of insulin resistance." Physiol Rev **84**(2): 623-647.

Naot, D. and J. Cornish (2008). "The role of peptides and receptors of the calcitonin family in the regulation of bone metabolism." Bone **43**(5): 813-818.

O'Brien, T. D., et al. (1994). "Islet amyloid polypeptide in human insulinomas. Evidence for intracellular amyloidogenesis." Diabetes **43**(2): 329-336.

O'Brien, T. D., et al. (1993). "Islet amyloid polypeptide: a review of its biology and potential roles in the pathogenesis of diabetes mellitus." Vet Pathol **30**(4): 317-332.

O'Brien, T. D., et al. (1986). "Immunohistochemical morphometry of pancreatic endocrine cells in diabetic, normoglycaemic glucose-intolerant and normal cats." J Comp Pathol **96**(4): 357-369.

O'Brien, T. D., et al. (1985). "High dose intravenous glucose tolerance test and serum insulin and glucagon levels in diabetic and non-diabetic cats: relationships to insular amyloidosis." Vet Pathol **22**(3): 250-261.

Ohlsson, H., et al. (1993). "IPF1, a homeodomain-containing transactivator of the insulin gene." EMBO J **12**(11): 4251-4259.

Oyadomari, S., et al. (2002). "Endoplasmic reticulum stress-mediated apoptosis in pancreatic beta-cells." Apoptosis **7**(4): 335-345.

Parks, J. K., et al. (2001). "Neurotoxic Abeta peptides increase oxidative stress in vivo through NMDA-receptor and nitric-oxide-synthase mechanisms, and inhibit complex IV activity and induce a mitochondrial permeability transition in vitro." J Neurochem **76**(4): 1050-1056.

Paulsson, J. F., et al. (2006). "Intracellular amyloid-like deposits contain unprocessed pro-islet amyloid polypeptide (proIAPP) in beta cells of transgenic mice overexpressing the gene for human IAPP and transplanted human islets." Diabetologia **49**(6): 1237-1246.

Paulsson, J. F. and G. T. Westermark (2005). "Aberrant processing of human proislet amyloid polypeptide results in increased amyloid formation." Diabetes **54**(7): 2117-2125.

Peiris, A. N., et al. (1989). "Relative contribution of obesity and body fat distribution to alterations in glucose insulin homeostasis: predictive values of selected indices in premenopausal women." Am J Clin Nutr **49**(5): 758-764.

Pelleymounter, M. A., et al. (1995). "Effects of the obese gene product on body weight regulation in ob/ob mice." Science **269**(5223): 540-543.

Perley, M. J. and D. M. Kipnis (1967). "Plasma insulin responses to oral and intravenous glucose: studies in normal and diabetic sujbjects." J Clin Invest **46**(12): 1954-1962.

Picarel-Blanchot, F., et al. (1996). "Impaired insulin secretion and excessive hepatic glucose production are both early events in the diabetic GK rat." Am J Physiol **271**(4 Pt 1): E755-762.

Pick, A., et al. (1998). "Role of apoptosis in failure of beta-cell mass compensation for insulin resistance and beta-cell defects in the male Zucker diabetic fatty rat." Diabetes **47**(3): 358-364.

Portha, B., et al. (2001). "beta-cell function and viability in the spontaneously diabetic GK rat: information from the GK/Par colony." Diabetes **50 Suppl 1**: S89-93.

Preston, A. M., et al. (2009). "Reduced endoplasmic reticulum (ER)-to-Golgi protein trafficking contributes to ER stress in lipotoxic mouse beta cells by promoting protein overload." Diabetologia **52**(11): 2369-2373.

Randle, P. J., et al. (1965). "The glucose fatty acid cycle in obesity and maturity onset diabetes mellitus." Ann N Y Acad Sci **131**(1): 324-333.

Sakagashira, S., et al. (1996). "Missense mutation of amylin gene (S20G) in Japanese NIDDM patients." Diabetes **45**(9): 1279-1281.

Scherz-Shouval, R. and Z. Elazar (2007). "ROS, mitochondria and the regulation of autophagy." Trends Cell Biol **17**(9): 422-427.

Schroder, M. (2008). "Endoplasmic reticulum stress responses." Cell Mol Life Sci **65**(6): 862-894.

Shafrir, E. and A. Gutman (1993). "Psammomys obesus of the Jerusalem colony: a model for nutritionally induced, non-insulin-dependent diabetes." J Basic Clin Physiol Pharmacol **4**(1-2): 83-99.

Shafrir, E., et al. (1999). "Nutritionally induced insulin resistance and receptor defect leading to beta-cell failure in animal models." Ann N Y Acad Sci **892**: 223-246.

Shang, F., et al. (1997). "Activity of ubiquitin-dependent pathway in response to oxidative stress. Ubiquitin-activating enzyme is transiently up-regulated." J Biol Chem **272**(37): 23086-23093.

Shaw, J. E., et al. (2010). "Global estimates of the prevalence of diabetes for 2010 and 2030." Diabetes Res Clin Pract **87**(1): 4-14.

Shimizu, M., et al. (1990). "Postmortem autolysis in the pancreas: multivariate statistical study. The influence of clinicopathological conditions." Pancreas **5**(1): 91-94.

Shprecher, D. R., et al. (2014). "Sustained remission of Parkinson disease associated melanoma with immunotherapy." Parkinsonism Relat Disord **20**(9): 1027-1029.

Shulman, G. I. (2000). "Cellular mechanisms of insulin resistance." J Clin Invest **106**(2): 171-176.

Sigal, R. J., et al. (2006). "Physical activity/exercise and type 2 diabetes: a consensus statement from the American Diabetes Association." Diabetes Care **29**(6): 1433-1438.

Small, D. H. and R. Cappai (2006). "Alois Alzheimer and Alzheimer's disease: a centennial perspective." J Neurochem **99**(3): 708-710.

Smeekens, S. P., et al. (1992). "Proinsulin processing by the subtilisin-related proprotein convertases furin, PC2, and PC3." Proc Natl Acad Sci U S A **89**(18): 8822-8826.

Smith, P. E., et al. (2009). "Induction of negative curvature as a mechanism of cell toxicity by amyloidogenic peptides: the case of islet amyloid polypeptide." J Am Chem Soc **131**(12): 4470-4478.

Soeller, W. C., et al. (1998). "Islet amyloid-associated diabetes in obese A(vy)/a mice expressing human islet amyloid polypeptide." Diabetes **47**(5): 743-750.

Stumvoll, M., et al. (2002). "Association of the T-G polymorphism in adiponectin (exon 2) with obesity and insulin sensitivity: interaction with family history of type 2 diabetes." Diabetes **51**(1): 37-41.

Tajiri, Y., et al. (1997). "Long-term effects of aminoguanidine on insulin release and biosynthesis: evidence that the formation of advanced glycosylation end products inhibits B cell function." Endocrinology **138**(1): 273-280.

Tesseur, I., et al. (2006). "Deficiency in neuronal TGF-beta signaling promotes neurodegeneration and Alzheimer's pathology." J Clin Invest **116**(11): 3060-3069.

Tomita, T., et al. (1992). "Pancreatic islets of obese hyperglycemic mice (ob/ob)." Pancreas **7**(3): 367-375.

Tremblay, A., et al. (1991). "Normalization of the metabolic profile in obese women by exercise and a low fat diet." Med Sci Sports Exerc **23**(12): 1326-1331.

Venters, H. D., et al. (2001). "Tumor necrosis factor(alpha) and insulin-like growth factor-I in the brain: is the whole greater than the sum of its parts?" J Neuroimmunol **119**(2): 151-165.

Wang, F., et al. (2001). "Islet amyloid develops diffusely throughout the pancreas before becoming severe and replacing endocrine cells." Diabetes **50**(11): 2514-2520.

Wang, J., et al. (2001). "The prohormone convertase enzyme 2 (PC2) is essential for processing pro-islet amyloid polypeptide at the NH2-terminal cleavage site." Diabetes **50**(3): 534-539.

Watada, H., et al. (1996). "Involvement of the homeodomain-containing transcription factor PDX-1 in islet amyloid polypeptide gene transcription." Biochem Biophys Res Commun **229**(3): 746-751.

Weir, G. C. and S. Bonner-Weir (2004). "Five stages of evolving beta-cell dysfunction during progression to diabetes." Diabetes **53 Suppl 3**: S16-21.

Weir, G. C., et al. (2001). "Beta-cell adaptation and decompensation during the progression of diabetes." Diabetes **50 Suppl 1**: S154-159.

Westermark, G. T., et al. (2000). "Islet amyloid development in a mouse strain lacking endogenous islet amyloid polypeptide (IAPP) but expressing human IAPP." Mol Med **6**(12): 998-1007.

Westermark, G. T., et al. (2000). "Pro islet amyloid polypeptide (ProIAPP) immunoreactivity in the islets of Langerhans." Ups J Med Sci **105**(2): 97-106.

Westermark, P., et al. (2011). "Islet amyloid polypeptide, islet amyloid, and diabetes mellitus." Physiol Rev **91**(3): 795-826.

Westermark, P., et al. (1995). "Rapid deposition of amyloid in human islets transplanted into nude mice." Diabetologia **38**(5): 543-549.

Westermark, P., et al. (1996). "Effects of beta cell granule components on human islet amyloid polypeptide fibril formation." FEBS Lett **379**(3): 203-206.

Westermark, P. and E. Wilander (1978). "The influence of amyloid deposits on the islet volume in maturity onset diabetes mellitus." Diabetologia **15**(5): 417-421.

Westwell-Roper, C., et al. (2011). "IL-1 blockade attenuates islet amyloid polypeptide-induced proinflammatory cytokine release and pancreatic islet graft dysfunction." J Immunol **187**(5): 2755-2765.

Whiting, D. R., et al. (2011). "IDF diabetes atlas: global estimates of the prevalence of diabetes for 2011 and 2030." Diabetes Res Clin Pract **94**(3): 311-321.

Wild, S., et al. (2004). "Global prevalence of diabetes: estimates for the year 2000 and projections for 2030." Diabetes Care **27**(5): 1047-1053.

Woerle, H. J., et al. (2008). "Impaired hyperglycemia-induced delay in gastric emptying in patients with type 1 diabetes deficient for islet amyloid polypeptide." Diabetes Care **31**(12): 2325-2331.

Wu, C. and J. E. Shea (2013). "Structural similarities and differences between amyloidogenic and non-amyloidogenic islet amyloid polypeptide (IAPP) sequences and implications for the dual physiological and pathological activities of these peptides." PLoS Comput Biol **9**(8): e1003211.

Xu, G., et al. (1998). "Insulin mediates glucose-stimulated phosphorylation of PHAS-I by pancreatic beta cells. An insulin-receptor mechanism for autoregulation of protein synthesis by translation." J Biol Chem **273**(8): 4485-4491.

Yagui, K., et al. (1995). "Formation of islet amyloid fibrils in beta-secretory granules of transgenic mice expressing human islet amyloid polypeptide/amylin." Eur J Endocrinol **132**(4): 487-496.

Zaidi, M., et al. (1990). "Amylin-amide: a new bone-conserving peptide from the pancreas." Exp Physiol **75**(4): 529-536.

Zhang, Y., et al. (2009). "Sphingomyelinase dependent apoptosis following treatment of pancreatic beta-cells with amyloid peptides Abeta(1-42) or IAPP." Apoptosis **14**(7): 878-889.

Acknowledgments:

I would like to thank Dr. Melania Osto and Prof. Thomas Lutz for their supervision and advices. I would also like to thank Neurimmune (Switzerland) for financially supporting the project and for providing the NI 203.26C11 antibody. Especially, I would like to thank Dr. Fabrice Heitz at Neurimmune who provided support, advices and specific feedbacks on the data. The financial support by the CTI (project # 13750.1 PFFLE-LS) is also gratefully acknowledged. A big thank you to all my colleagues for their help and for the great time spent together.

Curriculum Vitae

Last Name:	Durrer
First Name:	Alexandra
Date of birth:	30.10.1986
Place of birth:	Vevey
Nationality:	Swiss
School education :	07/2003, Collège secondaire de Vevey, Vevey, Switzerland
Secondary education:	06/2005 Matura Gymnase de Burier, La Tour-de-Peilz, Switzerland
Vet. Med. studies:	10/2005, Vetsuisse Fakultät, University of Bern, Switzerland
Graduation:	09/2011, Vetsuisse Fakultät, University of Bern, Switzerland
Working experience:	10/2011-10/2012, Veterinary assistant, Vetconcept SA, Lausanne, Switzerland 11/2013- currently, Veterinary assistant, Vetconcept SA, Lausanne, Switzerland
Dissertation:	11/2012-11/2013, Department of Veterinary Physiologie, Vetsuisse Fakultät, University of Zurich, Switzerland